


RESEARCH

Open Access



Preclinical study on *camellia sinensis* extract-loaded nanophytosomes for enhancement of memory-boosting activity: optimization by central composite design

Varsha Mane^{1,2*} , Suresh Killedar³, Harinath More¹ and Harshal Tare⁴

Abstract

Background The purpose of the present study was to enhance the memory-boosting activity of the standardized hydroalcoholic *Camellia sinensis* extract (CSE) by the formation of nanophytosomes with Leciva S70 phospholipid. The central composite design was used to optimize the solvent evaporation method for the formulation of *C. sinensis* phytosomes (CSP).

Results The optimized formulation had a mean particle size of $212.3 \text{ nm} \pm 0.39$, PDI of 0.238 ± 0.0197 , and zeta potential of $-42.02 \pm 0.995 \text{ mV}$. *C. sinensis* phytosome formation was confirmed by analytical techniques. The aqueous solubility of the developed CSP was 95.92 ± 0.31 , which is 7.34 times greater than that of pure CSE (13.07 ± 0.19). CSP was found more effective than either pure CSE ($26.42 \pm 0.4654\%$) or the physical mixture ($32.15 \pm 0.4596\%$) in releasing the CSE from the formulation ($72.16 \pm 0.5248\%$). Acute toxicity study corroborated the safety of CSP in rats. CSP demonstrated a significant ($p < 0.05$) reduction in escape and transferred latency on both days (15th and 16th) as compared to CSE, indicating the improvement of the memory-boosting activity. Furthermore, CSP-treated rats significantly improved acetylcholine (Ach) levels and brain tissue concentration compared with CSE. Moreover, the phytosomal formulation of CSP exhibited its rationality with an improvement of bioavailability by 3.21 folds compared with pure CSE.

Conclusion The presence of phospholipids in the CSP formulation and the formation of smaller particles may aid in crossing the blood–brain barrier, increasing brain tissue concentration and bioavailability. This, in turn, leads to an increase in memory-boosting activity.

Keywords *Camellia sinensis* extract, Phospholipid, Central composite design, Toxicity, Memory-boosting activity, Brain tissue

*Correspondence:

Varsha Mane
varsha.mane76@gmail.com

Full list of author information is available at the end of the article



© The Author(s) 2024. **Open Access** This article is licensed under a Creative Commons Attribution 4.0 International License, which permits use, sharing, adaptation, distribution and reproduction in any medium or format, as long as you give appropriate credit to the original author(s) and the source, provide a link to the Creative Commons licence, and indicate if changes were made. The images or other third party material in this article are included in the article's Creative Commons licence, unless indicated otherwise in a credit line to the material. If material is not included in the article's Creative Commons licence and your intended use is not permitted by statutory regulation or exceeds the permitted use, you will need to obtain permission directly from the copyright holder. To view a copy of this licence, visit <http://creativecommons.org/licenses/by/4.0/>.

Graphical abstract

Camellia sinensis extract

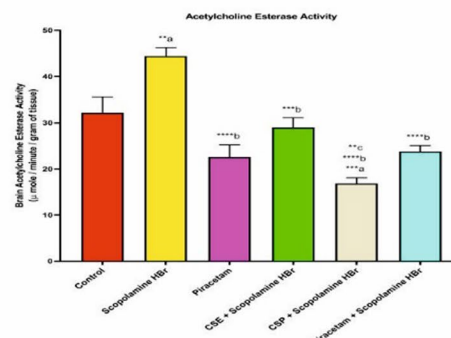
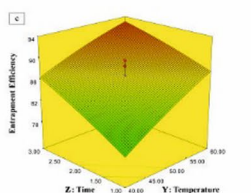
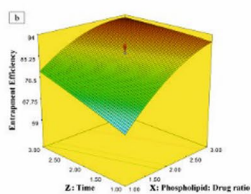
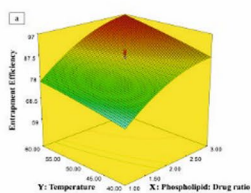


Preparation of *Camellia sinensis* phytosomes formulation

Estimation of Brain tissue concentration of pure extract and optimized formulation

Characterization

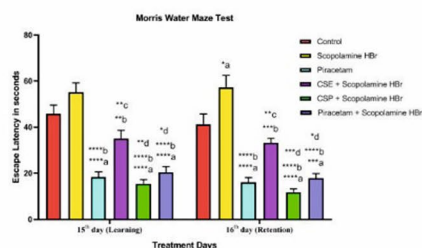
Histopathological study



Estimation of Acetylcholinesterase Activity in Rat's Brain



Acute toxicity study



Evaluation of *In vivo* Memory enhancing activity

Background

Neurodegenerative diseases are chronic, debilitating conditions marked by significant cognitive impairments, gradual death of neurons, and secondary abnormalities in the white matter tract [1]. Alzheimer's disease (AD) is a progressive, neurodegenerative brain disease that affects memory and other cognitive abilities over time. It causes dementia, behavioral changes, memory and thinking skill impairments, personality disorders, and diffuse anatomical abnormalities in the brain [2]. AD is characterized by the deposition of $\beta 1$ amyloid peptide plaque deposition, cholinergic cell loss, especially in the basal forebrain, and neurofibrillary tangles [3]. Acetylcholine (ACh), a neurotransmitter, is lost along with cholinergic cells. Dementia appears to be caused mainly by a decline in ACh in the brains of AD patients [4]. In 50 to 70% of cases, Alzheimer's dementia affects persons in their middle to late years. As people become older, the prevalence of AD doubles every five years after the age of 65.

Currently, individuals diagnosed with AD and other forms of dementia, such as transient ischemic episodes, stroke, organic brain disorders, mental retardation, and multi-infarct dementia, have limited pharmaceutical treatment alternatives at their disposal. The current therapies are essentially symptomatic; there has not been a noteworthy therapeutic breakthrough that prevents, modifies, or controls dementia and AD [5]. The most popular AChE inhibitors used to treat cholinergic deficiency in the brain are donepezil, rivastigmine, and galantamine; however, they have limitations such as a short duration of action, a low bioavailability, and a restricted therapeutic index [6]. Additionally, due to additional negative effects and non-specificity in the site of action, several synthetic drugs promoted as cognitive enhancers, including piracetam, amphetamine, pemoline, pyritinol, and others, are not safe for long-term use in humans. Their usage is also constrained by significant side effects such as hepatotoxicity [7]. Only one or two of every 10,000 of these chemical and synthetic compounds are clinically successful and safe enough for regulatory approval in the clinical process, despite the drawn-out development process. In reality, clinical trials for approximately half of all drug candidates fail. So considering these major drawbacks of synthetic molecules, many pharmaceutical firms are currently focusing on the development of plant-derived drug delivery systems [8].

Over the past decade, herbal and ayurvedic drugs from the plant kingdom have become a subject of world importance in neurodegenerative disorders with both medicinal and economic implications. Regular and widespread use of herbs throughout the world has increased serious concerns over their quality, safety, and efficacy. Thus, proper scientific evidence or assessment has

become the criteria for the acceptance of herbal health claims [9]. However, the scientific literature supporting the efficacy of herbal therapies is incomplete. Few well-controlled studies support the efficacy of herbal remedies in the treatment and clinical improvement of patients with neurodegenerative disorders like dementia, AD, and Parkinson's disease. Available scientific evidence has not yet confirmed the validity of their popular role in the treatment of these diseases [10]. The use of herbal medicine becoming popular due to the toxicity and side effects of allopathic medicines. Medicinal plants play an important role in the development of potent therapeutic agents.

The herbs acting on the brain are called Nootropic herbs and their isolated constituents are referred to as smart drugs. These herbs enhance memory as well as increase blood circulation in the brain. Different plants have been used as memory enhancers in folkloric medicine [11]. Therefore, it is necessary to prepare herbal formulations by using some reputed herbal sources as a memory enhancer. However, water-soluble phytoconstituents (like flavonoids, tannins, glycoside & aglycones, etc.) are poorly absorbed either due to their large molecular size which cannot absorb by passive diffusion or due to their poor lipid solubility; severely limiting their ability to pass across the lipid-rich biological membranes, resulting poor bioavailability [12]. Lipid solubility and molecular size represent the primary limiting factors for drug molecules to traverse biological membranes and achieve systemic absorption following oral or topical administration. The particle size reduction is achieved by using two novel techniques phytosomes and nanonization to easily pass through the blood-brain barrier for maintaining their concentration at the site of action [13, 14]. Standardized plant extracts or mainly polar phytoconstituents like flavonoids, terpenoids, tannins, and xanthenes when complexed with phospholipids like phosphatidylcholine give rise to a new drug delivery technology called phytosome (or herbosome) showing much better absorption profile following oral administration owing to improved lipid solubility which enables them to cross the biological membrane, resulting enhanced bioavailability at lesser dose [15, 16].

The *Theaceae* family includes the *C. sinensis* plant, generally referred to as the tea plant. It is a prominent medicinal herb in many indigenous medical systems, including Ayurveda, Unani, and homeopathy, and is utilized extensively by tribal people in China and India. Polyphenols, including (but are not limited to) catechin, gallocatechin, epicatechin, epigallocatechin, epicatechin gallate, and epigallocatechin gallate (EGCG), are found in *C. sinensis*, with EGCG having the highest concentration and being the most active

phytoconstituents. It contains alkaloids (caffeine, theobromine, and theophylline), polysaccharides, vitamins, volatile oils, and minerals [17]. It has many biological activities, including stimulant, diuretic, astringent, antioxidant, anticancer, anti-inflammatory, anti-obesity, antistress, hepatoprotective, cardioprotective, antiviral, antidiabetic, neuroprotective, gastrointestinal tract problem relieving activity, anti-inflammatory, analgesic, antipyretic, antiallergic, and skeleton muscle system reducing activity. These factors contribute to its enormous popularity. Green tea's potent effect on creating or lowering neurotransmitters, including acetylcholine, dopamine, and serotonin, all of which are involved in memory and learning, contributes to its ability to improve these processes [18, 19]. Polyphenols may also aid in the prevention and treatment of dementia [20].

The main objective of the present investigation was to increase the water solubility, bioavailability, and memory-enhancing activity of the standardized hydroalcoholic *C. sinensis* extract by forming a vesicular complex with Leciva S70 phospholipid in the form of phytosomes.

Material and methods

Materials

The standardized hydroalcoholic *C. sinensis* leaf extract was provided by Arjuna Remedies in Kerala. Leciva S70 (Phospholipid) was provided by VAV Life Sciences Pvt. Ltd, Mumbai Sigma-Aldrich supplied Epigallocatechin 3 gallate (EGCG), scopolamine HBr (hydrobromide), and piracetam. The dialysis membrane 60 was provided by Analab Fine Chemicals. Ethanol, methanol, n-octanol, and chloroform were furnished by Sigma-Aldrich Corporation. The rest of the materials were of superb analytical quality.

Methods

Preparation of *C. sinensis* phytosomes

The formulations for the *C. sinensis* leaf extract-loaded phytosomes (CSP) were developed using solvent evaporation techniques. 250-ml round-bottom flasks were filled with various ratios of *C. sinensis* extract (CSE) and Leciva S70 (1:1, 1:2, and 1:3). Then, 50 ml of ethanol was added to this. The reaction was conducted by maintaining the RBF-containing reaction mixture at different temperatures (40, 50, and 60 °C) for a predetermined time (1/2, 3 h), following the CCD. During heating, the reaction mixture was stirred. The solution was then evaporated and stored in a vacuum desiccator for a night to remove any trace of solvent that might have been left over after the initial incubation. The dry mixture was held in an amber bottle for later use [20].

Table 1 Experimental central composite design factors at three levels regions

| Central composite design (CCD) | Coded factors | Levels | | |
|---|---------------|--------|----|----|
| | | -1 | 0 | +1 |
| <i>Independent variables</i> | | | | |
| Phospholipid: drug ratio (% w/w) | X | 1 | 2 | 3 |
| Temperature (°C) | Y | 40 | 50 | 60 |
| Time (Hr) | Z | 1 | 2 | 3 |
| <i>Dependent variable: Entrapment efficiency in % (A)</i> | | | | |

Experimental design and statistics

The effects of independent parameters like drug ratio (% w/w), temperature (°C), and time (Hr), on entrapment efficiency (EE), were analyzed using central composite design (CCD), an optimization tool based on the response surface methodology. Using Design Expert 7.0.0 software, the experimental data were analyzed. Table 1 lists the levels of the considered independent variables and their experimental ranges for EE (% w/w).

Entrapment Efficiency (EE)

The efficiency of the developed phytosomes was assessed through a solvent extraction method as described previously. One hundred mg of the formulation was weighed and evenly dispersed throughout 10 ml chloroform. The produced phytosomes and Leciva S70 were dissolved in chloroform making CSE insoluble. The resulting mixture was centrifuged (Remi, Mumbai) at 5000 RPM. The sediment was removed from the transparent supernatant solution. Alcohol (ethanol) was used as the solvent in a UV/VIS spectrophotometer (UV 3000+, LAB INDIA) for non-aggregated CSE which showed a peak at 274 nm. Finally, a calibration curve was used to estimate the Epigallocatechin 3 gallate concentration using the $Y = 0.02275x + 0.017429$ regression equation.

Particle size

Particle size distribution and mean particle size of the optimized batch of CSP were determined at a constant temperature of 25 °C using Malvern Instrument, Malvern, UK (Model: ZEN 3600). The water was used to distribute the particles evenly. The polydispersity index (PDI) was used to determine the extent to which size distributions varied [21].

Zeta potential determination

The zeta potential was analyzed using the Scientific SZ-100 HORIBA (for Windows [Z Type] Ver2.40) analyzer. The optimum CSP formulation was tested for stability by zeta potential analysis. The average zeta

potential, charge, and mobility of optimized CSP were measured after 60 s of study [22].

FTIR spectroscopy

The FTIR spectra of CSE, physical mixture (PM), CSP, and Leciva S70 (phospholipid) were obtained using an FTIR-7600 (Lambda Scientific) spectrophotometer. All samples were dried in a hot air oven at 50 °C for two hours to remove moisture. Each sample (~1 mg) was evenly mixed with potassium bromide (approximately 100 mg), then compressed at a pressure of 10 Ton/nm² to form a disk-shaped pellet. The resulting pellet was placed inside the sample container and scanned from 4000 to 500 cm⁻¹ at a resolution of 4 cm⁻¹.

Powder X-ray diffraction (XRD)

The polymorphic states of CSE, Leciva S70, PM, and CSP were investigated utilizing a powder X-ray diffractometer (Model: D8 Advance, Bruker AXS, USA) equipped with a Bragg–Brentano geometry ($\theta/2$) optical setup to record X-ray diffraction patterns. The samples were scanned between 3 and 60 degrees, with a setup angle range of between 0.2 and 2 θ and a count time of 0.5 s.

Solubility analysis

The solubility of CSE, PM, and CSP was determined by using the method already described [23]. Briefly, the excessive amount of samples was dissolved in either water or n-octanol (10 ml) in airtight glass containers at room temperature (25 °C). The glass bottles containing the solutions were shaken with an orbital shaker (RIV-OTTEK) for 24 h and centrifuged for 20 min at 4000 RPM (REMI, India). The clear supernatant was isolated and passed through a membrane filter (0.45 μ). 1 ml of this filtrate was then diluted appropriately and analyzed at 274 nm using a UV/ VIS spectrophotometer (UV 3000+, LAB INDIA).

In Vitro release studies

The in vitro release of CSE, PM, and CSP was performed using a dialysis membrane (MW cut off > 12,000 KDa). Before filling the samples, the dialysis membrane was soaked in distilled water for 1 min. Fifty mg of CSE was dissolved in a buffer solution (4 ml) to form a suspension. Under the same conditions, an equivalent amount of CSP was dispersed into to buffer solution. The dialysis bag was filled with the prepared dispersions and tied from both ends. The dialysis membrane bag containing the sample was suspended in a mixture of phosphate-buffered saline (PBS) (200 ml, pH 7.4) and Tween 20 (1% w/v) in a glass beaker. The buffer solution was stirred under magnetic stirring at 100 RPM maintaining a temperature of

37 \pm 0.5 °C. The samples (5 ml) were withdrawn at a pre-determined time interval and replenished with an equal volume of freshly prepared buffer to maintain the sink condition. The aliquots were filtered using a 0.45-micron membrane filter before being measured at 274 nm (Telange et al. 2017) using a UV/VIS spectrophotometer (UV 3000+, LAB INDIA). In addition to these studies, we have performed Differential scanning calorimetry (DSC), Scanning electron microscopy (SEM), Proton Nuclear Magnetic Resonance and stability study. The detailed experimental methods of these studies is provided in Additional file 1.

Acute toxicity study

All animal handlings and experiments were approved by the Animal Ethical Committee of Crystal Biological Solution, Pune, with approval number CRY/2122/070. Acute toxicity testing was performed on healthy, non-pregnant, and nulliparous female Wistar rats. Four experimental groups of 12 female rats ($n=3$) were formed. Groups I and II were given CSP formulations at 300 mg/kg bw, while groups III and IV received 2000 mg/kg bw. The dose titration was done with the population from each group's safety in mind. The Wistar rats were starved for three hours before and after the dosage. Throughout the trial, water was available at all times. Individual animals were monitored for the first 30, 60, 120, 180, and 240 min following treatment and once a day for the next 14 days [24].

Dosing and sampling schedule

For the in vivo memory-enhancing activity investigation, 36 Wistar rats of both sexes (male and female) weighing 175–240 gm were employed. The animals were divided into six groups each containing 6 in each groups. As per CPCSEA guidelines, rats were provided with free access to food and water and kept in an animal house with standard laboratory conditions (constant room temperature (25 \pm 2 °C), relative humidity (50–70% RH), and a 12-h light/dark cycle). Carboxymethyl cellulose (CMC) 0.5% (10 ml/kg bw) was administered to Group I (Control) for 15 days, (Negative control) Scopolamine HBr (0.4 mg/kg bw) was received to Group II (Negative control) by i.p. route on the 15th day. In Group III (the Positive control group), subjects were given piracetam orally at a regular dose (200 mg/kg body weight) for 15 days. Group IV received an oral dose of *C. sinensis* extract (CSE) (250 mg/kg bw) for 15 days, followed 45 min later by an i.p injection of scopolamine HBr (0.4 mg/kg bw). After 15 days of oral administration of CSP formulation (equal to 250 mg/kg bw of CSE), scopolamine HBr (0.4 mg/kg bw) was injected (i.p.) after 45 min of CSP

formulation administration in Group V, 15 days of oral piracetam (200 mg/kg bw) were followed by 45 min of injection (i.p) of scopolamine HBr (0.4 mg/kg bw) in Group VI.

In 0.5% (w/v) CMC solution, CSE, CSP, and piracetam solutions were produced. All animals were treated according to the schedule and exposed to a behavioral analysis study. Simultaneously, the same groups were employed for three different models. Animals were pre-treated with MWMT, EPMT, and PCT on alternating days before the tests. On day 15, 90 min following the administration of the relevant dose, the transfer latency (TL)/ or the escape latency (EL) was determined. Both of these measurements took place. After 24 h had passed since the last session, the retention of all learned tasks was assessed [25].

In vivo memory-enhancing/boosting activity

In this study, the term “memory-enhancing/boosting activity” means to elevate the memory and cognitive functions which were determined using various behavioral tests including Morris Water Maze Test, Elevated Plus Maze Test, Pole Climbing Test, and the measured outcomes like escape latency, transfer latency, acetylcholine, serotonin, and dopamine levels. The memory-enhancing efficacy of optimized CSP in contrast to CSE was compared.

Elevated plus maze test

Using an exteroceptive behavioral paradigm, the EPMT was utilized to examine the effects of training on rat memory and learning (where the stimulus was external to the body). The apparatus had two bare arms (each 50 cm×10 cm) and two covered arms (each 50 cm×40 cm×10 cm). Extending the arms from a central platform, the maze was raised to 50 cm from the floor (10 cm×10 cm). On day one, the rats were placed one by one at the very tip of the open arm, with their backs to the platform in the middle. The rat's opposite gender was identified in any covered areas to see if the test rat's retentive memory caused it to go quicker toward that region. The TL was determined by recording the time it took the rat to move inside any of the covered arms containing the opposing gender while using all four of its legs. On the first day, each animal's TL was noted. Within the first 90 s, the animal was allowed to enter one of the covered arms. If it did not, it was coaxed into gently entering one of the arms. A time limit of 90 s was imposed there. After the rat had explored the maze for ten more seconds, it was put back in its cage. The retention of this learned task was evaluated 24 h after the last dose or on day 16 of treatment. A considerable decrease in the TL value of retention showed memory improvement [26].

Morris water maze test

The MWMT was performed in a circular swimming pool of 100 cm in diameter and 50 cm in height. The circular pool was built with filling and draining facilities and installed on a framework with the water level at waist height. The circular tank's floor was divided into four equal quadrants. Up to a depth of 30 cm of water was added. One of the pool's four corners has a plastic platform dug 2 cm below the water's surface (9 cm in diameter and 28 cm in height). The milk was used to make the pool opaque. The trial platform was consistently situated in the same spot.

The rats were trained to swim without a platform on the first day of the test. Then, after a brief introduction, the animals were released into the tank and given 10 s to explore the exhibit, including sitting on the secret platform. After 90 s, if the rat still had not found the platform, it was placed on it and left there for 10 s. On alternating days, rats were trained for 15 days. The trial was successful when the rat sat on the hidden platform within 90 s. If rats spend more than three minutes looking for the hidden platform, that is a mistake. Throughout the investigation, the experimental setting remained the same. Memory improvement was indicated by a considerable fall in the EL value [27].

Pole climbing test

The cognitive processes of learning and memory retention were studied using Cook's pole climbing equipment. The apparatus consists of a soundproof experimental chamber (25×25×25 cm) with a floor grid. The chamber's floor grid is made of stainless-steel rods. The chamber's floor grid received a scrambled shock (6 mA). A hole at the room's center top was used to suspend a pole with a diameter of around 2.5 cm. Wistar rats were placed in the chamber and given 45 s to investigate their surroundings. The buzzer served as the conditioned stimulus (CS), and the 45 s of electrical shock through the grid floor served as the unconditioned stimulus (US). Once the animal connected the sound of the buzzer to the impending foot shock, it could avoid the pain by climbing the pole after the signal was given. A record of the EL quantity was kept. The animals were initially screened using this paradigm, and only those who exhibited an escape response on at least one of the trials were included [26].

Estimation of acetylcholinesterase activity in rat's brain

On the 16th day, after conducting MWMT, EPMT, and PCT, Five Wistar rats from each group were anesthetized by giving an intramuscular injection (Ketamine Hydrochloride IP) and decapitated. Instantaneously after removal, the brains were washed in icy saline and frozen at -80°C for later use. 0.1 M phosphate buffer (pH 8.0)

was used to homogenize the tissue after measuring its weight (0.1 gm of tissue per ml of phosphate buffer). Two and a half milliliters of buffer and one hundred microliters of DTNB 5,5-dithio bis (2-nitrobenzoic acid) were placed in a cuvette. Then, 4 ml aliquots of the homogenate were added. The resulting mixture was well mixed, and the absorbance was measured in a photometric calorimeter at 412 nm. After recording the basal measurement, 20 ml of the substrate (i.e., acetylthiocholine) was added to the solution mentioned above when the absorbance reached a steady value. The change in absorbance was measured every two minutes for 10 min. [27].

Estimation of dopamine concentration in Rat's brain

DA GENLISA™ ELISA kit was used for the quantitative determination of dopamine in Wistar rat brain homogenate solution by sandwich ELISA technique. Fifty µl of prepared rat dopamine (DA) standard solutions of 0.3, 0.6, 1.2, 2.4, 4.8, and 9.6 ng/ml was added to respective standard wells. These standard solutions were used for the construction of the calibration curve. Forty µl of Wistar rat brain homogenate sample solution from groups I to VI was added to respective sample wells. Ten µl of biotinylated DA antibody was added to the respective sample wells. The biotinylated DA antibody was not added to standard wells because the standard solution contains the biotinylated antibody. Fifty µl of streptavidin-HRP conjugate was added to all sample wells. Mixed well. The plate was covered with a sealer and incubated for 60 min at 37 °C. The plate was aspirated, washed four times with diluted wash buffer (1X), and the residual buffer was blotted by firmly tapping the plate upside down on absorbent paper. Wipe out all liquid from the bottom outside of the microtiter wells, as any residue can interfere with the reading step. Fifty µl TMB Substrate A was added followed by 50 µl TMB Substrate B in all the wells. The plate was covered and incubated at 37 °C for 10 min. The wells had turned bluish. Fifty µl of stop solution was added to all wells. The wells were turned from blue to yellow. Absorbance was recorded at 450 nm with a microplate reader within 10–15 min after the addition of the stop solution [28].

Estimation of serotonin concentration in rat's brain

The Rat Serotonin, ST GENLISA™ ELISA kit was used for the quantitative determination of serotonin in Wistar rat brain-homogenated solution by sandwich ELISA technique. Fifty µl of prepared serotonin (ST) standard solutions of 7.5, 15, 30, 60, 120, and 240 ng/ml was added to respective standard wells. These standard solutions were used for the construction of the calibration curve. Forty µl of Wistar rat brain homogenate sample solution from groups I to VI were added to respective

sample wells. Ten µl of biotinylated ST antibody was added to the respective sample wells. The biotinylated ST antibody was not added to standard wells because the standard solution contains the biotinylated antibody. Fifty µl of streptavidin-HRP conjugate was added to the respective sample wells and also the standard wells. The streptavidin-HRP conjugate was not added to the blank well. Mixed well. The plate was covered with a sealer and incubated for 60 min at 37 °C. The plate was aspirated and washed four times with diluted wash buffer (1X), and the residual buffer was blotted by firmly tapping the plate upside down on absorbent paper. Wipe out all liquid from the bottom outside of the microtiter wells, as any residue can interfere with the reading step. Fifty µl TMB Substrate A was added, followed by 50 µl TMB Substrate B in all the wells. The plate was covered and incubated at 37 °C for 10 min. The wells had turned bluish. Fifty µl of stop solution was added to all wells. The wells were turned from blue to yellow. Absorbance was recorded at 450 nm with a microplate reader within 10–15 min after the addition of the stop solution [29].

Histopathological study

One animal from each group received an intramuscular dose of Ketamine Hydrochloride IP at the end of the treatment session, rendering it unconscious so that its brain could be dissected. The removed brain was stored in a 10% (v/v) formalin solution. A hematoxylin and eosin reagent was used to stain between 3- and 5-µ-thick sections. The brain slices were studied with an optical microscope, and pictures were taken with the microscope's attached digital camera at a magnification of 400x.

Procedure for estimation of the concentration of CSE and CSP in brain tissue

The concentration of CSE and CSP in brain tissue was determined using a brain-homogenated solution (4 ml) from animal groups IV and V. The homogenized brain solutions were placed into two distinct 5-ml centrifuge tubes and spun for 15 min at 10,000 rpm. CSE and CSP clear supernatants were separated and used for HPLC analysis.

High-Performance liquid chromatography (HPLC)

Epigallocatechin 3 gallate was used as a marker to estimate the CSE and CSP in brain tissue. A bioanalytical HPLC (Model: Waters 2695 alliance) approach was developed for the Epigallocatechin 3 gallate marker. A Zorbax SB C18 5µ (4.6×150) mm column was utilized. This experiment was conducted using the chromatographic gradient technique. As a mobile phase, water with 0.1% (v/v) formic acid and acetonitrile (ACN) with 0.08% (v/v) formic acid were

observed. Mobile phase filtration was performed using a 0.45- μ m millipore filter. The mobile phase flow rate was maintained at 1.0 ml/min, and the column temperature was held at 30°C. At 274 nm, a PDA-type detector was utilized [30]. (Regression Equation: $Y=44,929.71 X-4900.50$ and Retention time: 7.417 Minutes).

Comparative pharmacokinetic study of CSP and CSE in the blood plasma compartment

18 Wistar albino rats (both sexes) weighing between 240 and 370 g were used in the pharmacokinetic study. Wistar albino rats were housed in a standard laboratory setting and provided free access to food and water as per CPCSEA guidelines. For the study, animals were fasted overnight until 2 h after medication and then given food. Animals were divided into three groups containing six in each group. Group I (Control): 0.5% (w/v) CMC solution (10 ml/kg bw), Group II: CSE (250 mg/kg bw and Group III: CSP formulation (equivalent to 250 mg/kg bw of CSE). CSP and CSE were dissolved individually in a 0.5% (w/v) CMC solution and given to the different groups orally. All Wistar rats were anesthetized with Ketamine Hydrochloride IP (intramuscular injection). The retro-orbital vein was punctured to collect blood samples (0.5–0.7 ml) and collected in Eppendorf tubes at intervals of 0, 0.5, 1, 2, 3, 4, 6, 8, 12, and 24 h. Plasma was separated using centrifugation (Remi, Mumbai, India) at 10,000 rpm for 10 min, and the sample was then frozen at -40°C for further drug analysis [31].

Preparation of plasma samples for HPLC analysis

One ml of purified plasma and 2 ml of methanol were placed in the centrifuge tube. After 30 s of vigorous agitation, centrifugation at 10,000 rpm for 10 min, and collection of the clear supernatant, the tube was discarded. The protein-free solution was stored in a tube at -40°C in the freezer until HPLC analysis was done.

Estimation of pharmacokinetic parameters

A protein-free clear supernatant (20 μ l) was put into the chromatographic system that had been designed. The calculated concentration at each time was based on the obtained peak area. Then, directly from plasma concentration–time data estimated by one extravascular compartment model using PK Solver, the pharmacokinetic parameters (maximum plasma concentration) C_{max} , (area under the concentration–time curve) AUC, (corresponding time) t_{max} , (half-life, clearance) CL/F, and (volume of distribution) V/F were calculated.

Results

Preparation of CSP and statistical analysis of EE

Table 2 summarizes all the formulation batches as per CCD with independent and dependent variables. Table 3 summarizes the model statistics suggesting a quadratic model.

Based on the proposed model, the following polynomial quadratic equation was predicted

$$\% EE = 87.06 + 9.37 X + 4.02 Y + 3.45 Z + 0.83 XY - 2.65 XZ - 0.74 YZ - 4.08 X^2 - 0.43 Y^2 - 0.31 Z^2$$

The positive sign suggested a favorable effect on the reaction, while the negative sign indicated the opposite. Table 4 displays the ANOVA results for the quadratic model of the response surface.

The model F value was found to be 48.66, making it statistically significant. A model F value this large could only have occurred by chance 0.01% of the time. There is only a 0.01% chance that a model F value this large is due to noise. The likelihood of error value ($\text{prob} > F$) was then used to evaluate the significance of each model term. If “ $\text{prob} > F$ ” is less than 0.0500, then the model terms are significant; if it is more than 0.1000, they are not significant. Based on the F values, all three independent factors substantially impacted the EE of the developed phytosomes. When controlling for factors like temperature and time, the phospholipid-to-drug ratio (%w/w) was the most crucial factor in EE (%). It has also been found that the phospholipid: drug ratio and temperature positively affected EE (%). The lack-of-fit test indicated that independent variables have a considerable effect on the response if their value is insignificant. Nonsignificant lack of fit, however, is good. The lack-of-fit F score of 1.72 indicates that the lack of fit is not statistically significant compared to the total error. R^2 value, which measures how well a model fits data, was calculated to be 0.9777, indicating that the model has a good fit. The corrected R^2 value of 0.9576 agrees reasonably well with the expected value of 0.8812 for the same variable. The signal-to-noise ratio is the standard by which accuracy is judged. It is preferable if the ratio is higher than 4. In this scenario, the signal-to-noise ratio of 25.039 was satisfactory [32]. They also prove the model's utility for steering one's way through the design process. 3D response surface plots are shown in Fig. 1 and indicate a strong influence of the studied factors X, Y, and Z on the EE. Increasing levels of X, Y, and Z were found to be favorable conditions for obtaining higher EE.

Table 2 Three independent factors central composite design matrix and corresponding entrapment efficiencies from the experiment

| CCD batches | Factor X Phospholipid: drug ratio (% w/w) | Factor Y Temperature (°C) | Factor Z Time (Hr) | Response Entrapment efficiency (%) |
|-------------|---|------------------------------|-----------------------|--|
| 1 | 1 | 40 | 1 | 62.11 ± 0.95 |
| 2 | 3 | 40 | 1 | 83.14 ± 1.01 |
| 3 | 1 | 60 | 1 | 70.06 ± 1.36 |
| 4 | 3 | 60 | 1 | 94.41 ± 1.33 |
| 5 | 1 | 40 | 3 | 77.09 ± 0.97 |
| 6 | 3 | 40 | 3 | 87.50 ± 0.92 |
| 7 | 1 | 60 | 3 | 82.05 ± 0.98 |
| 8 | 3 | 60 | 3 | 95.81 ± 1.04 |
| 9 | 0.32 | 50 | 2 | 59.15 ± 1.06 |
| 10 | 3.68 | 50 | 2 | 93.90 ± 1.15 |
| 11 | 2 | 33.18 | 2 | 80.22 ± 0.99 |
| 12 | 2 | 66.82 | 2 | 93.51 ± 1.38 |
| 13 | 2 | 50 | 0.32 | 82.94 ± 1.06 |
| 14 | 2 | 50 | 3.68 | 91.48 ± 1.33 |
| 15 | 2 | 50 | 2 | 88.56 ± 1.44 |
| 16 | 2 | 50 | 2 | 86.68 ± 0.77 |
| 17 | 2 | 50 | 2 | 86.71 ± 0.96 |
| 18 | 2 | 50 | 2 | 85.02 ± 1.21 |
| 19 | 2 | 50 | 2 | 89.61 ± 0.86 |
| 20 | 2 | 50 | 2 | 85.42 ± 1.29 |

The data are shown as the Mean ± Standard Deviation (n = 3)

Table 3 Summarized data from the model statistics

| Source | SD | R ² | Adjusted R ² | Predicted R ² | PRESS | Comment |
|-----------|----------|----------------|-------------------------|--------------------------|----------|-----------|
| Linear | 4.675979 | 0.818925 | 0.784973 | 0.696805 | 585.7707 | |
| 2FI | 4.670834 | 0.8532 | 0.785446 | 0.612729 | 748.2049 | |
| Quadratic | 2.076719 | 0.977677 | 0.957587 | 0.881202 | 229.517 | Suggested |
| Cubic | 2.090348 | 0.98643 | 0.957028 | -0.1948 | 2308.345 | Aliased |

Validation of the Model

An additional batch of the CSP formulation was formulated and tested for model validation. The EE of the optimized batch was found to be 94.75 ± 1.06%, which is very near to the model predicted value, confirming the validity and applicability of the suggested model. The percentage bias was estimated using the following equation and was found to be 1.82, less than 3%, confirming the model’s relative robustness [33].

$$\text{Bias (\%)} = \frac{\text{Predicted value} - \text{Observed value}}{\text{Predicted value}} \times 100.$$

Particle size

The particle size of the optimized formulation was determined to be 212.3 nm ± 0.39 and is exhibited in Fig. 2a. The polydispersity index (PDI) for the optimized formulation was found to be 0.238 ± 0.0197.

Zeta potential

The zeta potential is another critical parameter used to evaluate the stability of the formulation and is shown in Fig. 2b. The optimized formulation obtained after preparation was measured to have a zeta potential of -42.02 ± 0.995 mV.

Table 4 Analysis of variance data revealing how different factors affect the EE

| Source | Sum of squares | df | Mean square | F Value | p value Prob > F | Comment |
|------------------------------------|----------------|----|-------------|----------|------------------|-----------------|
| Model | 1888.865 | 9 | 209.8738 | 48.66342 | <0.0001 | Significant |
| X-Phospholipid: drug ratio (% w/w) | 1199.546 | 1 | 1199.546 | 278.1387 | <0.0001 | |
| Y-Temperature | 220.2219 | 1 | 220.2219 | 51.06282 | <0.0001 | |
| Z-Time | 162.3877 | 1 | 162.3877 | 37.65281 | 0.0001 | |
| XY | 5.561113 | 1 | 5.561113 | 1.289454 | 0.2826 | |
| XZ | 56.23301 | 1 | 56.23301 | 13.03874 | 0.0048 | |
| YZ | 4.425312 | 1 | 4.425312 | 1.026097 | 0.335 | |
| X ² | 240.3307 | 1 | 240.3307 | 55.72545 | <0.0001 | |
| Y ² | 2.639323 | 1 | 2.639323 | 0.611979 | 0.4522 | |
| Z ² | 1.349202 | 1 | 1.349202 | 0.312839 | 0.5882 | |
| Residual | 43.12764 | 10 | 4.312764 | | | |
| Lack of fit | 27.27864 | 5 | 5.455727 | 1.721158 | 0.2829 | Not significant |
| Pure error | 15.849 | 5 | 3.1698 | | | |
| Cor total | 1931.992 | 19 | | | | |

Fourier transform infrared spectroscopy (FTIR)

The FTIR spectra of CSE, Leciva S70, Physical mixture (PM) of CSE and Leciva S70, and CSP are shown in Fig. 3 (from a to d). In CSE spectra, (a) peak appeared at 3417.96 cm^{-1} , representing OH stretching vibration for intermolecular hydrogen bonding substituted on a cyclic ringed structure left to the peak at 2925.48 cm^{-1} due to C-H stretching in Alkanes. The presence of a peak due to C-O stretching at 1238.08 cm^{-1} because of conjugation of the oxygen with the ring, along with the presence of a peak at 1342.21 cm^{-1} due to O-H in planer bending absorption, confirmed the phenolic structure. The presence of a peak at 1629.55 cm^{-1} and 1452.14 cm^{-1} due to aromatic C=C stretching and 1693.19 cm^{-1} due to C=O stretching confirmed the presence of the carbonyl is in conjugation with the aryl group. Generally, the C=O group from ketone appears in the range of 1720–1708 cm^{-1} for simple aliphatic ketone. Still, this band shifted to a lower frequency (1700–1680 cm^{-1}) when the C=O group was in conjugation with the phenyl or aryl group. C-N stretching absorption occurred at 1093.44 cm^{-1} in CSE.

FTIR spectra of pure Leciva S70 (b) revealed a peak at 3415.32 due to OH stretch. The peak appeared at 2925.48 cm^{-1} and 2856.06 cm^{-1} (C-H stretching present in the long fatty acid chain), 1743.33 cm^{-1} (C=O stretch in the fatty acids), 1236.15 cm^{-1} (P=O stretch), 1093.44 cm^{-1} (P-O-C stretch) and 970.02 cm^{-1} ($-\text{N}^+(\text{CH}_2)_3$ stretch).

PM FTIR spectra (c) showed peaks that were characteristics of CSE and Leciva S70 phospholipid at 3415.32, 3010.34, 2929.34, 2856.06, 1737.55, 1631.48, 1463.71, 1230.36, 1087.66, and 968.09 cm^{-1} .

The FTIR spectra of CSP formulation (d) exhibited a broad peak at 3403.03 cm^{-1} (intermolecular hydrogen bonded O-H stretch), 2925.48 cm^{-1} (intense peak related to CSE due to C-H stretch), 1743.33 (C=O stretch), 1625.70 and 1461.78 (due to C=C stretching in the aromatic ring), 1193.72 (P=O stretching), 1093.44 cm^{-1} (P-O-C stretch) and 973.88 cm^{-1} ($-\text{N}^+(\text{CH}_2)_3$ stretch).

Powder X-ray diffraction

Figure 4 shows CSE, Leciva S70, PM, and CSP x-ray diffraction patterns. CSE was found to be crystalline because its diffraction pattern showed several strong, sharp peaks, and one relatively broad peak. The presence of several sharp peaks and one relatively broad peak in the diffraction pattern is indicative of a crystalline material, as described by Andersan et al. [34]. Peaks for crystallinity in CSE were observed at 2θ values of 9.5, 12.45, 14.29, 24.14, 30.79, 34.20, 35.98, and 38.83°. Leciva S70 phospholipid exhibited two small and relatively broad peaks at 2θ values of 5.6, 7.5, and 20.27°, respectively. The physical mixture (PM) diffractogram presented few crystalline peaks with lower intensity than CSE and two peaks associated with Leciva S70 at 2θ values of 7.6, 9.47, 12.48, 19.93, 30.76, and 34.23°. Possible causes for the diminished crystalline peak strength include the in situ production of partial aggregates between CSE and Leciva S70, a decrease in the amount of CSE in the sample, and interference from the Leciva S70 molecule.

Solubility analysis

The solubility tests were performed on CSE, PM, and CSP using water and octanol. The lipophilic character

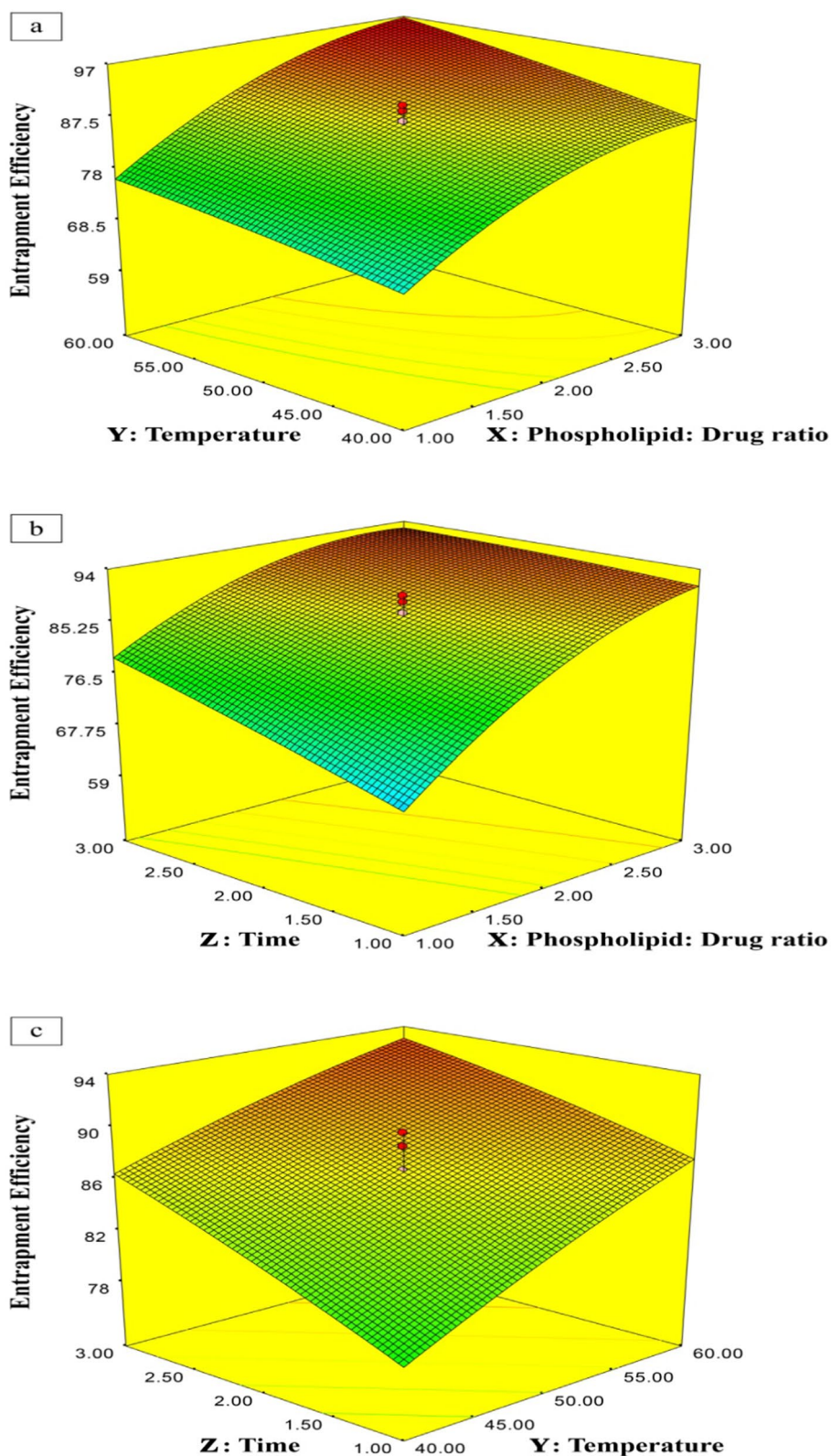


Fig. 1 Three-dimensional surface response plot showing the interactive effect of **a** Phospholipid: Drug ratio and Temperature, **b** Phospholipid: Drug and Time, and **c** Temperature and Time on EE

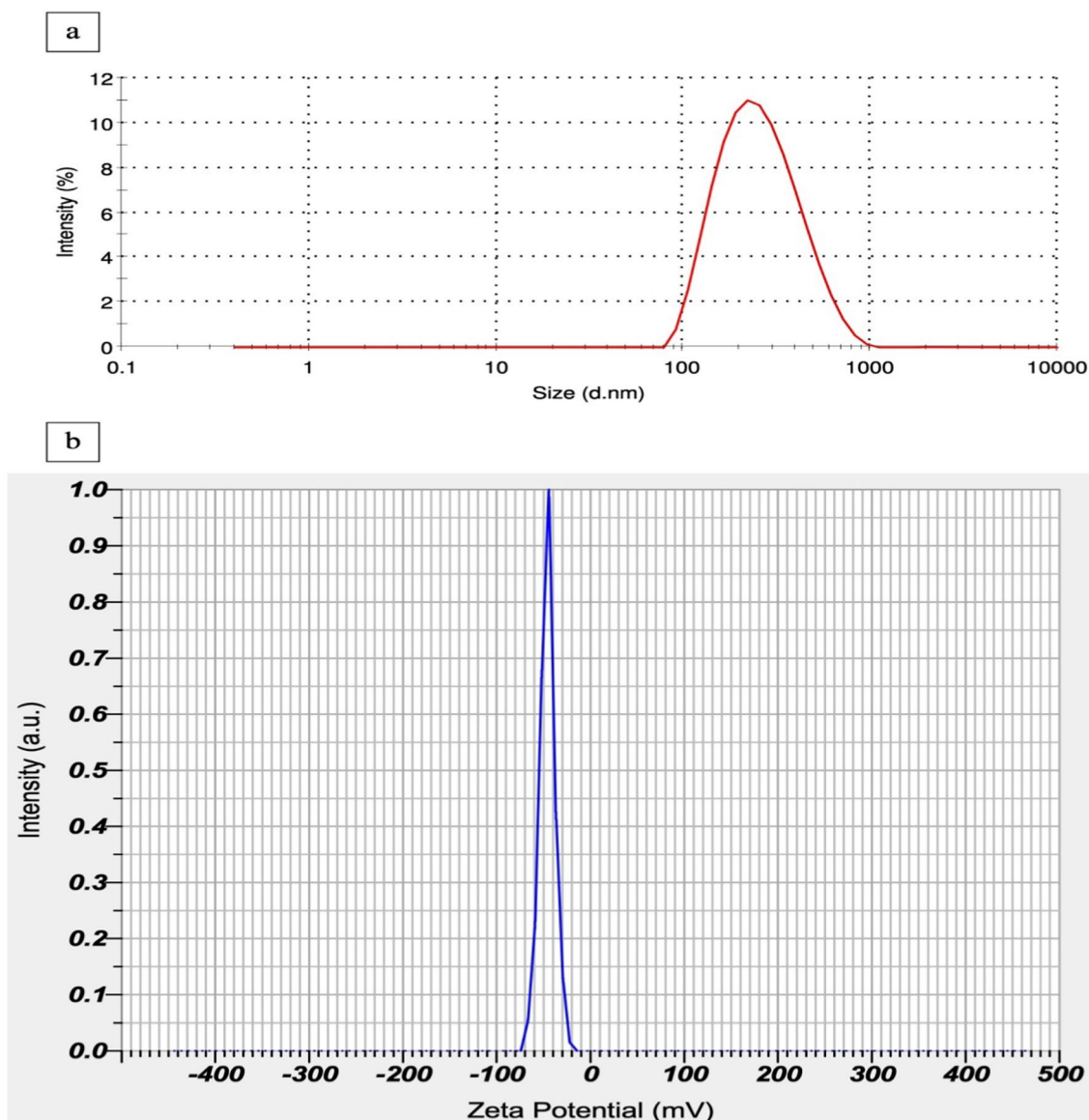


Fig. 2 a Particle size distribution and b Zeta potential of optimized CSP

of CSE was demonstrated by its lower aqueous solubility ($13.07 \pm 0.19 \mu\text{g/ml}$) and comparatively higher n-octanol solubility ($383 \pm 2.00 \mu\text{g/ml}$). Compared to the CSE, the physical mixture (PM) had 1.74 times higher aqueous solubility but no significant difference in n-octanol solubility. On the other hand, CSP had a much higher aqueous solubility (7.34 times) than CSE ($p < 0.05$).

In vitro release study

Results of in vitro release of CSE, PM, and CSP are shown in Fig. 5. The release profiles of CSE and PM were found to be identical and nonsignificant throughout the study

period. The release profile of CSE after 12 h was found to be $26.42 \pm 0.4654\%$, and for PM, it was $32.15 \pm 0.4596\%$. CSP followed a similar release pattern as CSE and PM during the initial 20 min. However, CSE’s release from CSP significantly increased and reached $72.16 \pm 0.5248\%$ after 12 h. In addition to these results few study results are provided in additional file 1. Differential scanning calorimetry (DSC) result is presented in Fig. S1. Scanning electron microscopy (SEM) results is shown in Fig. S2 and Proton Nuclear Magnetic Resonance data presented in Fig. S3. Also, the stability study result of the CSP formulation is shown in Table S1.

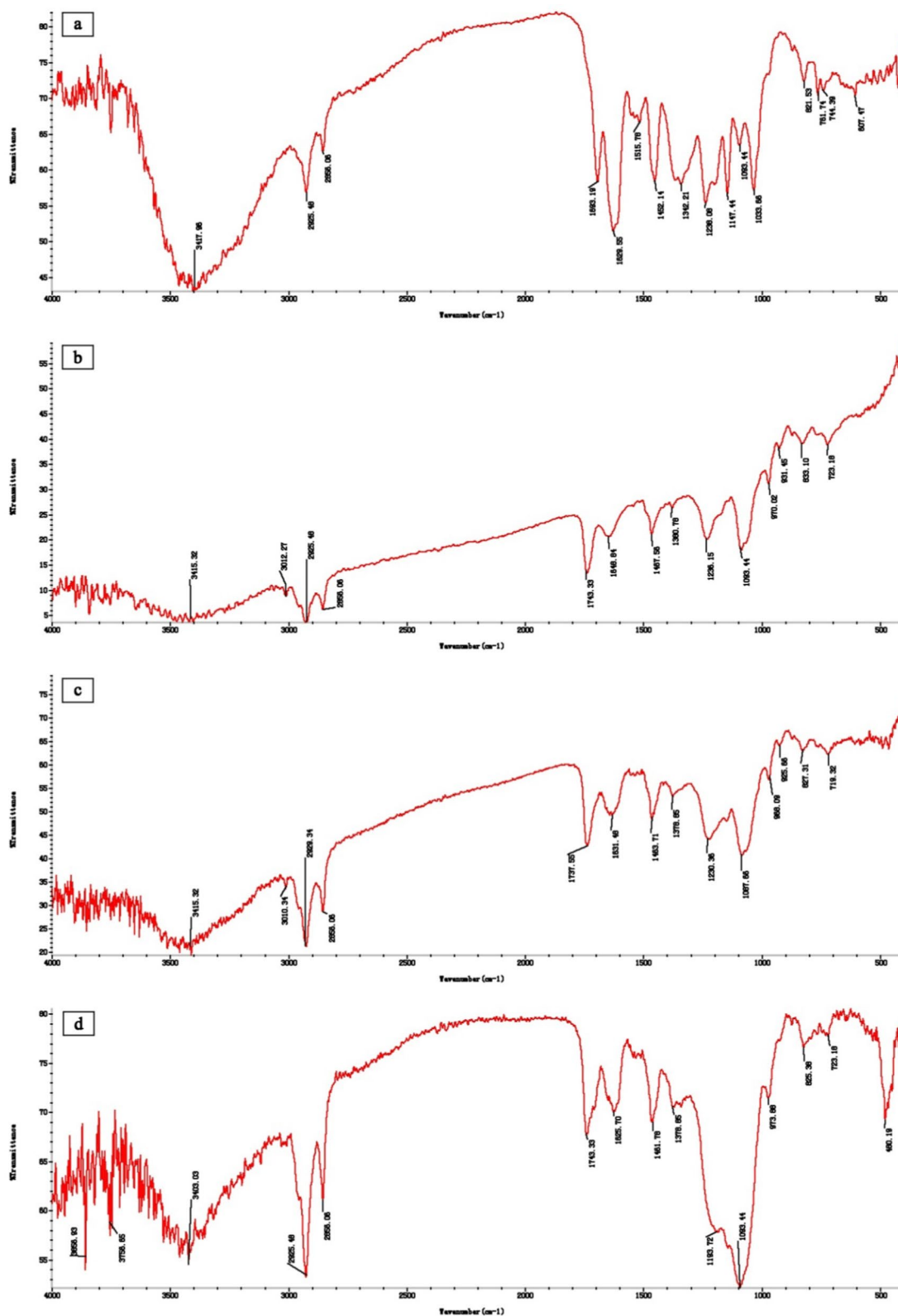


Fig. 3 FTIR spectra of **a** CSE, **b** Leciva S70, **c** PM, and **d** CSP

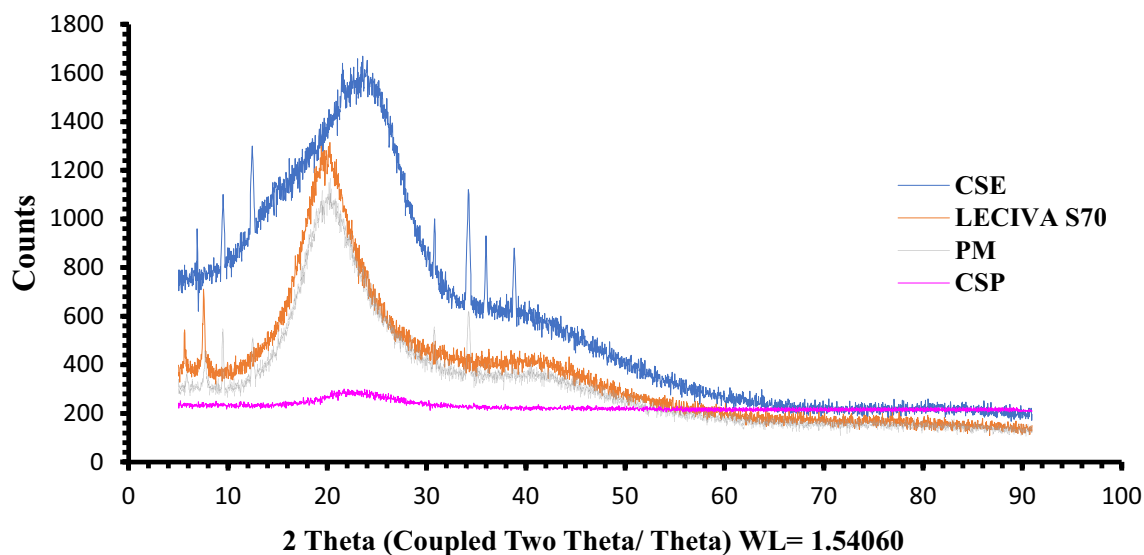


Fig. 4 XRD overlay spectra of CSE, PM, Leciva S70, and CSP

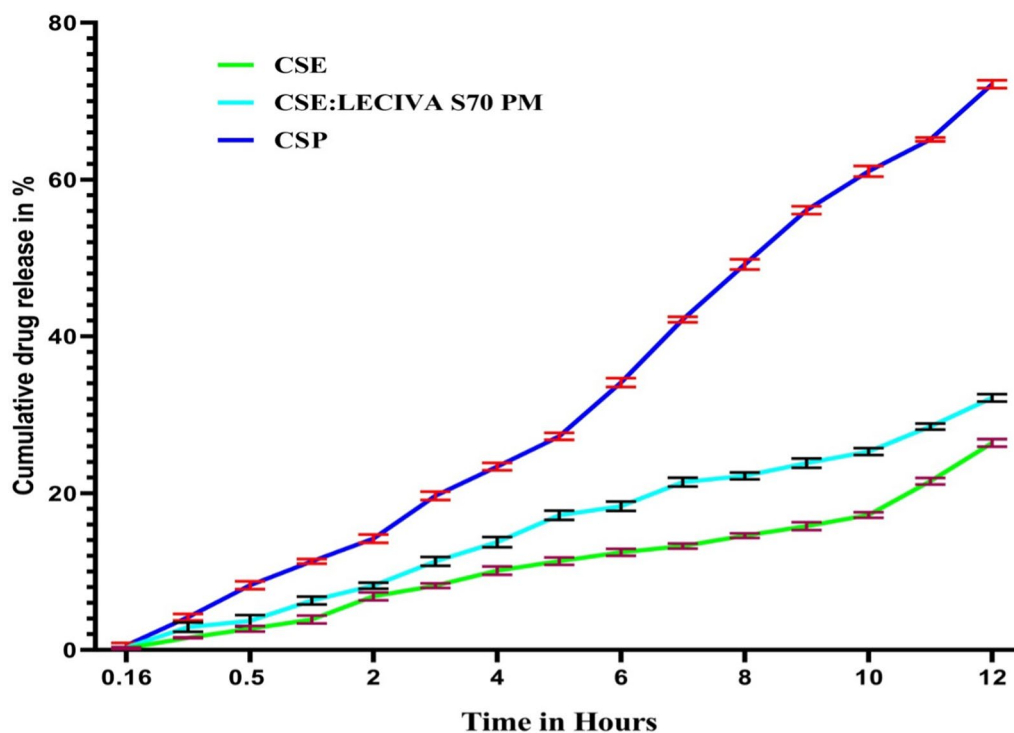


Fig. 5 In vitro drug release of CSE, PM, and CSP (The data are shown as the Mean ± Standard Deviation = 3)

Acute toxicity study

Female rats administered 300, and 2000 mg/kg bw of a CSP formulation showed no signs of death. Furthermore, all the animals did not show any clinical signs of toxicity immediately after dosing and appeared normal for up to 4 h.

In vivo memory-enhancing activity

EL/TL on the first day (i.e., the 15th day of drug treatment) reflected the acquisition of learning behavior, and the second day (i.e., the 16th day) reflected the retention of knowledge or memory in the animals. Evidence of memory enhancement was seen in a statistically

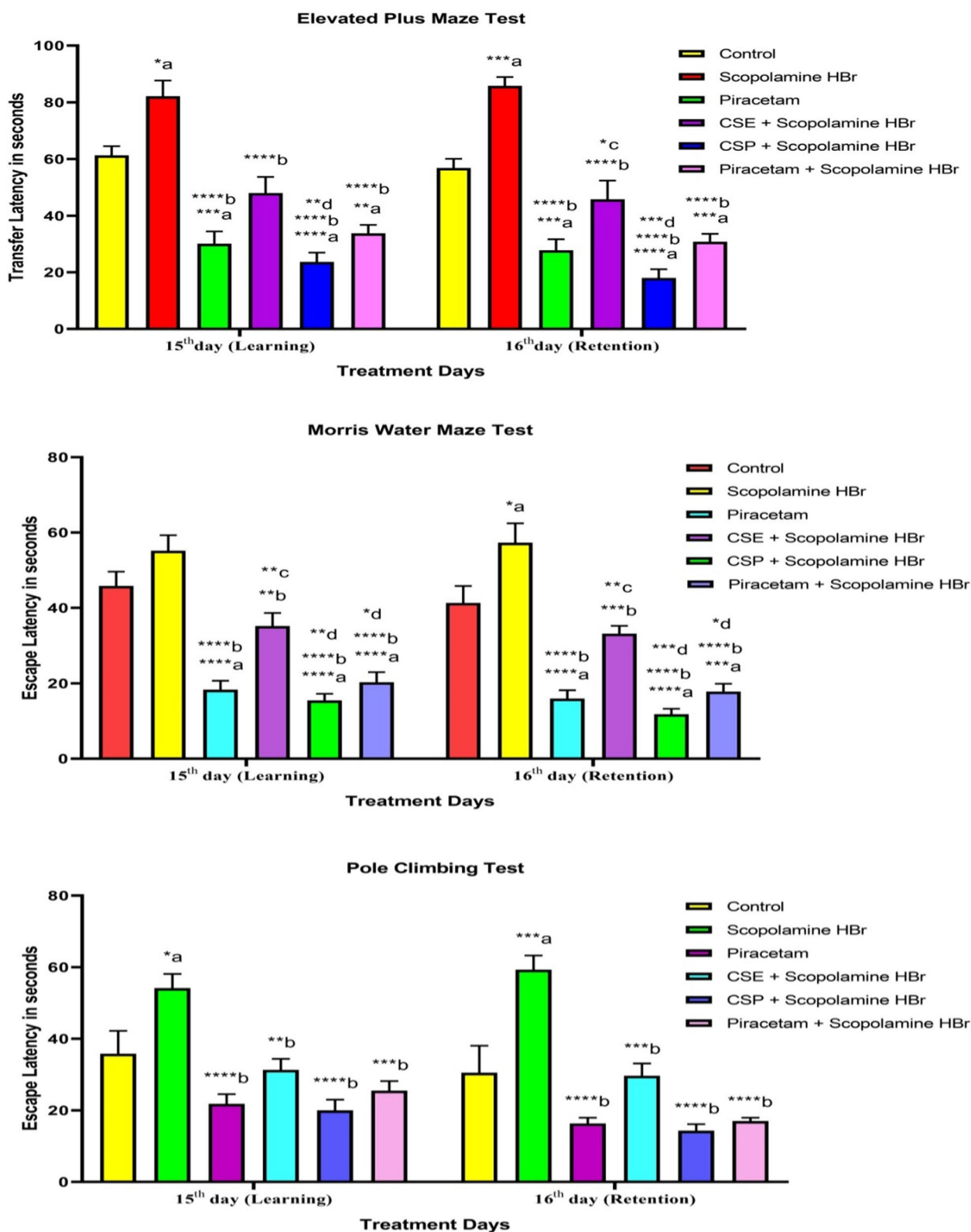


Fig. 6 Effect of CSE and CSP on spatial learning and memory in the a) EPMT, b) MWM, and c) PCT. Data are expressed as Mean ± SEM values (n=6 in each group). **a**=compared to a vehicle-treated normal control group; **b**=compared to the scopolamine HBr-treated group; **c**=compared with the piracetam-treated group; and **d**=compared with CSE + scopolamine HBr-treated group. (*p < 0.05, **p < 0.01, ***p < 0.001, ****p < 0.0001) (one-way ANOVA followed by Tukey's multiple comparisons test)

significant ($p < 0.05$) drop in EL and TL values. The findings of an *in vivo* investigation on memory enhancement can be seen in Fig. 6(a–c).

Elevated Plus Maze Test

TL parameter (in seconds) was measured in EPMT. The reduction in TL was considered to be a memory improvement. The results of EPMT are shown in Fig. 6a. The animal group administered with scopolamine HBr showed a significant increase in TL ($p < 0.05$) on the 15th and ($p < 0.001$) on the 16th day compared with the vehicle-treated control group. The piracetam, CSP+scopolamine HBr, and piracetam+scopolamine HBr-treated group revealed a significant reduction in TL ($p < 0.001$, $p < 0.0001$, and $p < 0.01$) on the 15th day and ($p < 0.001$, $p < 0.0001$ and $p < 0.001$) on 16th day respectively when compared to vehicle-treated group. A significant reduction in TL ($p < 0.0001$) on both days was found in piracetam, CSE+scopolamine HBr, CSP+scopolamine HBr, and piracetam+scopolamine HBr-treated groups when compared to scopolamine HBr-treated group. When CSE+scopolamine HBr was compared to the piracetam-treated group, an increase in TL ($p < 0.05$) was noticed. CSP+scopolamine HBr-treated group showed a significant decrease in TL ($p < 0.01$) on the 15th day and ($p < 0.001$) on the 16th day compared to the CSE+scopolamine HBr-administered group. Overall, there was a significant decrease in TL of CSP formulation administered in animals compared to all groups.

Morris water maze test

The results of MWMT are shown in Fig. 6b. On day 16, EL was higher in the scopolamine HBr group ($p < 0.05$) compared to the control group. On days 15 and 16, EL was considerably ($p < 0.0001$) lower in the piracetam and CSP+scopolamine HBr-treated animal group compared to the control and scopolamine HBr-administered animal group. The CSE+scopolamine HBr-administered group exhibited a decrease in EL ($p < 0.01$) on the 15th and ($p < 0.001$) on the 16th day as compared to the scopolamine HBr-treated group. When the CSE+scopolamine HBr group was compared with the piracetam-treated group, it was observed that EL ($p < 0.01$) significantly increased on both days, i.e., the 15th and 16th day. When the EL of the CSP+scopolamine HBr group was compared to that of the CSE+scopolamine HBr group, a statistically significant drop was found on day 15 ($p < 0.01$) and day 16 ($p < 0.001$). The group given piracetam+scopolamine HBr had a significantly lower EL when compared to the control, scopolamine HBr, and CSE+scopolamine HBr-treated groups ($p < 0.0001$, $p < 0.0001$, and $p < 0.05$) on the 15th day and ($p < 0.001$, $p < 0.0001$,

and $p < 0.05$) on the 16th day, respectively. However, the CSP+scopolamine HBr-treated group reduced EL significantly compared with CSE+scopolamine HBr, piracetam, and piracetam+scopolamine HBr-administered groups [26].

Pole climbing test

In the Pole Climbing Test, EL is the amount of time it takes the animal to ascend to avoid a foot shock following the sound of a buzzer. The reduction in EL (in seconds) was considered a memory improvement. The results of PCT are shown in Fig. 6c and found that the scopolamine HBr-administered group increased EL on the 15th ($p < 0.05$) and ($p < 0.001$) on the 16th day when compared with a control-treated group. Compared to scopolamine HBr-treated rats, piracetam and CSP+scopolamine HBr showed a statistically significant reduction in EL ($p < 0.0001$) on both days. Both CSE+scopolamine HBr and piracetam+scopolamine HBr resulted in lower EL levels 15 days after administration ($p < 0.01$, $p < 0.001$) and 16 days after administration ($p < 0.001$, $p < 0.0001$). It was noticed that the CSP formulation-treated group revealed a significant reduction in EL as compared to pure extract. In the case of all treated groups except scopolamine HBr, no significant increase or decrease in EL was observed compared to the control group on both days [26].

Acetylcholine esterase activity

CSE and CSP were tested for their influence on brain Ach esterase activity in scopolamine HBr-induced Wistar rats. The results are depicted in Fig. 7. For this study, we evaluated Ach esterase activity using one-way ANOVA, then Tukey's multiple comparison test. Compared to the control group that received the vehicle, the scopolamine HBr group showed a statistically significant ($p < 0.01$) increase in Ach esterase activity. This leads to a decrease in Ach transmitter level due to the breakdown of Ach by activated Ach esterase enzyme. A significant ($p < 0.001$) reduction in Ach esterase activity was seen in the CSP+scopolamine HBr-treated group compared to the control group. Compared to the vehicle-treated control group, Ach esterase activity was not significantly different in any treatment groups besides those receiving scopolamine HBr and CSP+scopolamine HBr. Treatment with piracetam, CSP+scopolamine HBr, piracetam+scopolamine HBr, or CSE+scopolamine HBr significantly reduced Ach esterase activity ($p < 0.0001$, $p < 0.0001$, $p < 0.0001$, $p < 0.001$) and increased Ach level at the cholinergic synapse compared to scopolamine HBr administration. Animals who were given CSP+scopolamine HBr showed a more significant reduction in acetylcholine esterase activity ($p < 0.01$) than those given CSE+scopolamine HBr group.

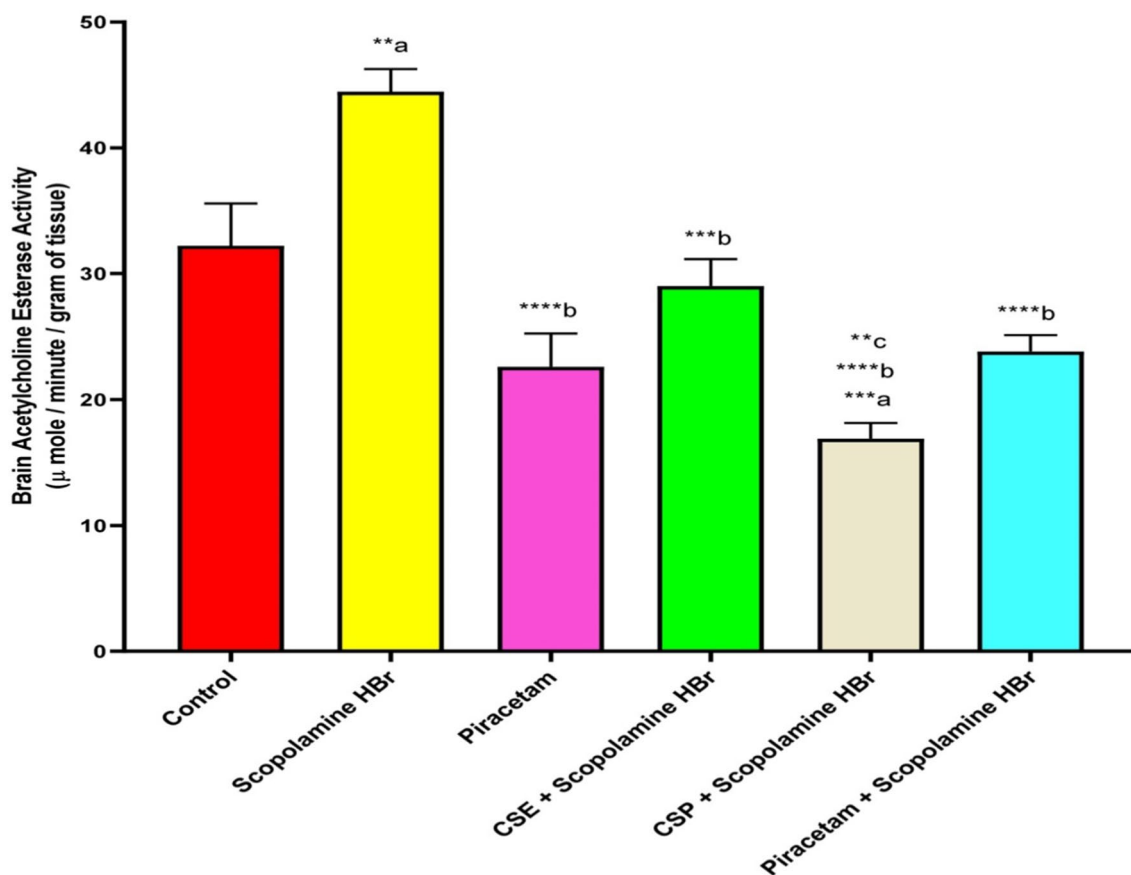


Fig. 7 Effect of CSE and CSP on brain Ach esterase activity in scopolamine-induced Wistar rats. Data are shown as the Mean \pm SEM values ($n=5$ in each group). **a**=compared to the vehicle-treated normal control group, **b**=compared to the scopolamine HBr-treated group and **c**=compared to the CSE + scopolamine HBr-treated group (* $p < 0.05$, ** $p < 0.01$, *** $p < 0.001$, **** $p < 0.0001$) (one-way ANOVA followed by Tukey's multiple comparisons test)

Estimation of dopamine concentration in Rat's Brain

The brain dopamine estimation was carried out by sandwich ELISA, and one-way ANOVA followed by Tukey's multiple comparison tests was used for the evaluation of dopamine level. The brain dopamine concentration level is shown in Fig. 8. The brain dopamine concentration was significantly increased in the piracetam and CSP-scopolamine HBr-treated groups ($p < 0.01$) when compared to the control. Piracetam and CSE-scopolamine HBr, CSP-scopolamine HBr, and piracetam-scopolamine HBr-treated groups showed significantly increased in dopamine level ($p < 0.0001$, $p < 0.05$, $p < 0.0001$, $p < 0.05$) compared to scopolamine HBr-treated group. When the CSP-scopolamine HBr-treated group was compared with the CSE-scopolamine HBr-treated group, we found a significantly increased dopamine level ($p < 0.05$). The brain dopamine concentration was found to be 18.07 ± 1.790 and 11.60 ± 1.718 ng/ml in the CSP and pure extract-treated groups, respectively.

Estimation of serotonin concentration in rat's brain

The brain serotonin level was determined by sandwich ELISA techniques. The result is exhibited in Fig. 9. A one-way ANOVA followed by Tukey's multiple comparison tests was used for the evaluation of serotonin levels. There was a significantly increased level of serotonin in piracetam, CSE-scopolamine HBr, CSP-scopolamine HBr, and piracetam-scopolamine HBr ($p < 0.0001$, $p < 0.01$, $p < 0.0001$, $p < 0.01$) compared to the control group. Brain serotonin levels were significantly increased ($p < 0.0001$) in all groups when compared to the scopolamine HBr-treated group. There has been a significantly increased level of serotonin ($p < 0.0001$) in the CSP formulation-treated group when compared to the CSE-scopolamine HBr-treated group. The brain serotonin concentration was found to be 47.92 ± 1.690 and 36.99 ± 1.742 ng/ml in the CSP formulation and pure extract-treated groups respectively.

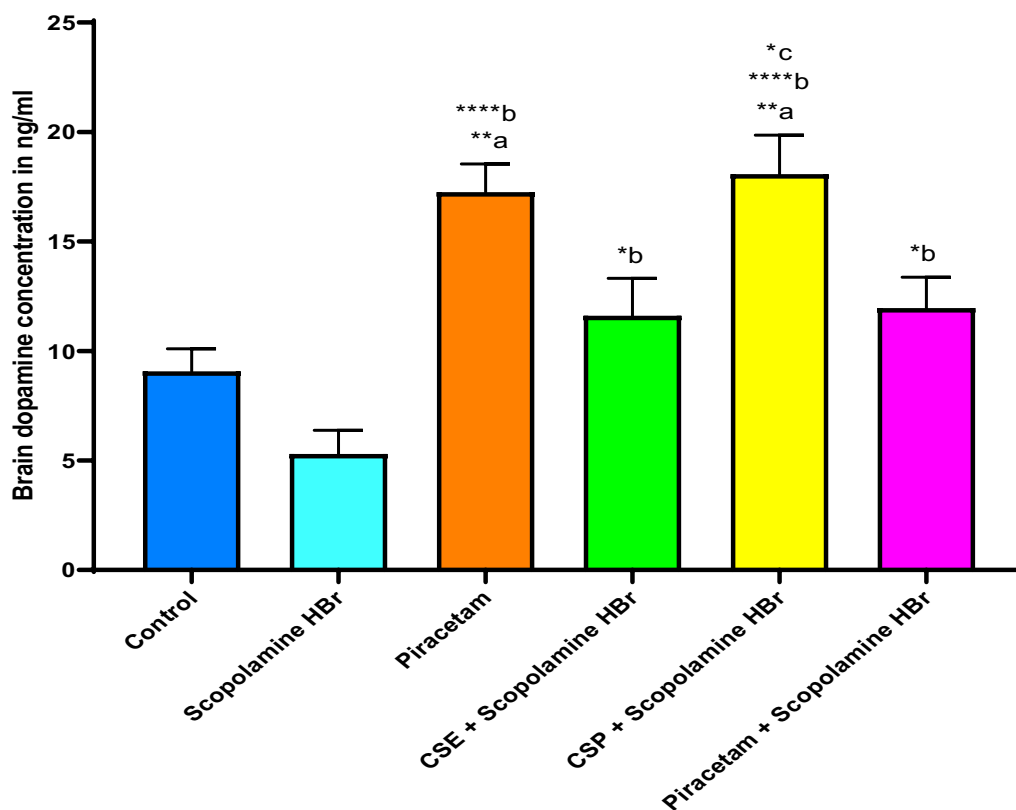


Fig. 8 Brain dopamine concentration level. Data are expressed as Mean \pm SEM values ($n=5$ in each group). **a**= compared to a vehicle-treated normal control group; **b**= compared to the scopolamine HBr-treated group; **c**= compared with CSE + scopolamine HBr-treated group. (* $p < 0.05$, ** $p < 0.01$, *** $p < 0.001$, **** $p < 0.0001$) (one-way ANOVA followed by Tukey's multiple comparisons test)

Histopathological study

The results of the histopathological examination of the brain are shown in Fig. 10. The normal control group did not exhibit any toxicity in terms of neuronal and vascular degeneration or glial cell infiltration (Fig. 10a). Moderate vascular deterioration, cerebral neuronal degeneration, necrosis, and glial cell infiltration were all observed in the brain of the disease-control animal (Fig. 10b). However, other animals belonging to different treatment groups showed mild pathological changes when compared with disease control. A mild type of glial cell infiltration and neuronal and vascular degeneration was observed in the piracetam (Fig. 10c) and CSE (Fig. 10d) administered group. The brains of CSP-treated animals showed only mild neuronal and vascular degeneration and glial cell infiltration as compared to CSE-treated group (Fig. 10e).

Estimation of the concentration of CSE and CSP in brain tissue

CSE and CSP concentrations were measured in given animals over 15 days and were found to be 1.143 ± 0.045 $\mu\text{g/ml}$ and 2.683 ± 0.21 $\mu\text{g/ml}$, respectively.

Comparative pharmacokinetic study of CSE and CSP in the blood plasma compartment

Table 5 displays the pharmacokinetic parameters that were determined using the PK Solver software. The results of the research showed that C_{max} , T_{max} , and $\text{AUC}_{0-\infty}$ were significantly higher ($p < 0.05$) in animals given CSP as compared to those given CSE. Additionally, a longer absorption half-life was found for CSP. The fact that the CL/F and V/F were significantly ($p < 0.05$) lower in the CSP-administered group mice compared to the CSE-treated animals provided additional support for CSP's longer residency and duration of effect.

Discussion

C. sinensis phytosomes were formulated by a solvent evaporation method using Leciva S70 as a phospholipid at varying phospholipid: drug ratio, temperature, and time. The effects of these independent variables were determined on the EE of *C. sinensis* extract. In the optimization study, the optimal criterion was the achievement of maximum EE at specific concentrations of the three independent variables. The optimum response

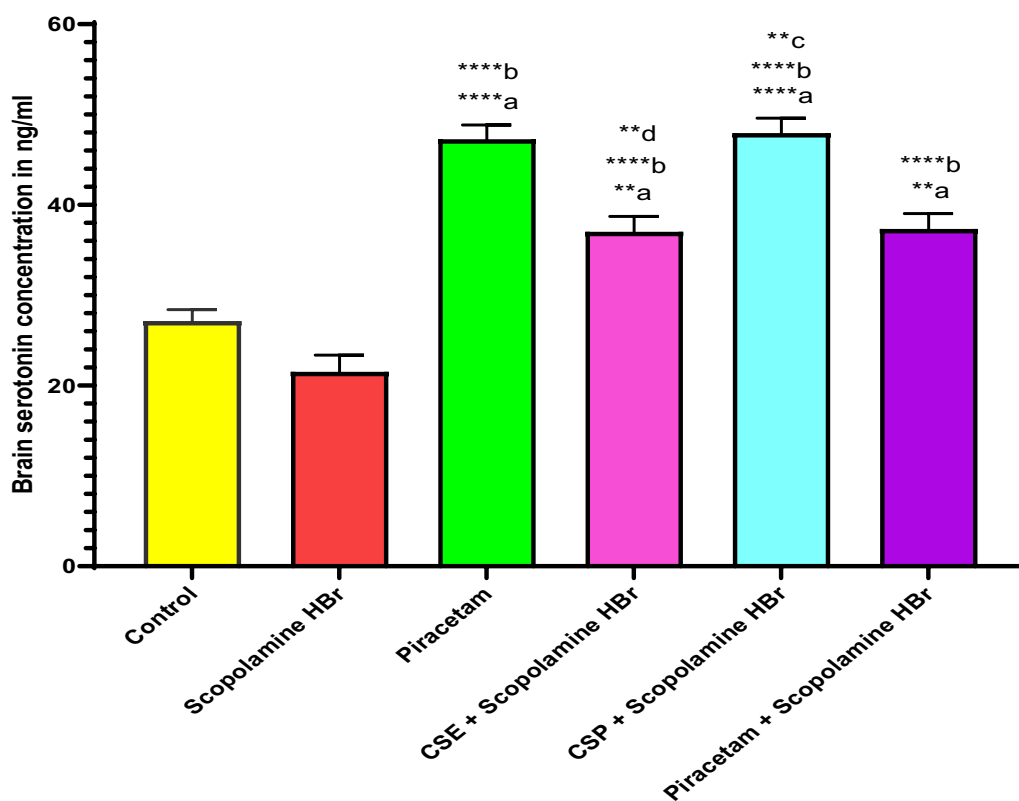


Fig. 9 Brain serotonin concentration level. Data are expressed as Mean \pm SEM values (n=5 in each group). **a**=compared to a vehicle-treated normal control group; **b**=compared to the scopolamine HBr-treated group; **c**=compared with CSE+scopolamine HBr-treated group, **d**=compared to piracetam-treated group. (* $p < 0.05$, ** $p < 0.01$, *** $p < 0.001$, **** $p < 0.0001$) (one-way ANOVA followed by Tukey's multiple comparisons test)

of EE was reported to be 96.51% at phospholipid: drug concentration of 3% w/w, at a temperature of 60 °C, and time of 3 h using the desirability function, with good desirability of 1. The particle size of the phytosomes is quite an important parameter that needs to be considered during the development of formulations. Particle size significantly influences the distribution of the formulation within tissues and organs. It has been noted that the average particle size for drug distribution to the brain and other organs ranges from approximately 100 to about 1000 nm, with the precise value contingent upon the dosage form and administration method. A PDI value of up to 0.3 is considered to be acceptable. It suggests a homogeneous population of phospholipid vesicles, which is desirable in lipid-based drug delivery applications like liposome and nanoliposome formulation [35]. Values of zeta potential greater than -30 mv are considered as satisfactory and indicative of solid physical stability. Phospholipid type and structure determine the zeta potential value. This indicated that the developed CSP formulation had good physical strength due to its nanometer particle size, low PDI, and moderate zeta potential value [36].

When FTIR spectra of CSP were compared with CSE and Leciva S70 phospholipid spectra, it was observed that the OH stretching frequency of CSE at 3417.96 cm^{-1} changed to 3403.03 cm^{-1} in the CSP formulation indicated the presence of weak intermolecular interactions. The CSE peaks at 1033.66, 1147.44, 1238.08, and 1342.21 cm^{-1} were found to be disappeared and appeared to be new broad doublet strong peak at 1093.44 (similar to the peak of Leciva S70 but more intense as compared to Leciva S70) and 1193.72 cm^{-1} . The absorption frequency and intensity of peak at 1629.55 cm^{-1} in CSE appeared too shortened along with a slight change in absorption frequency in CSP formulation and found at 1625.70 cm^{-1} . In CSE and Leciva S70 FTIR spectra, a tiny peak was observed at 1093.44 cm^{-1} , which appeared strong and intense in the CSP formulation and indicated the presence of interaction. The changes in absorption frequencies of peaks in CSP formulation compared to CSE and Leciva S70 revealed the presence of weak intermolecular interaction between CSE and Leciva S70 phospholipid may be the reason for the formation of CSP [37, 38]. X-ray diffraction study was used to identify the

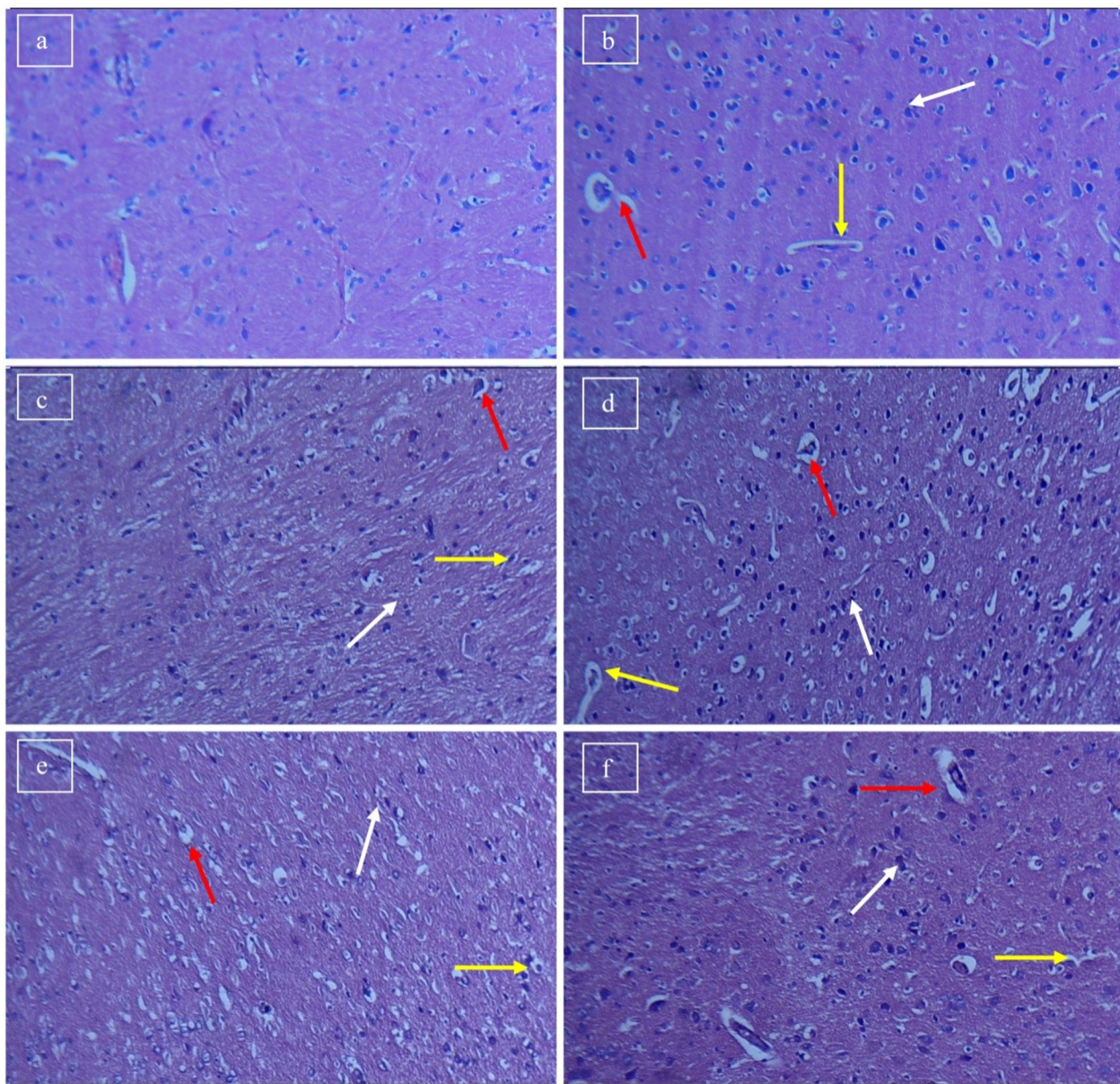


Fig. 10 Histopathology micrographs of rat brain **a**) Group I, **b**) Group II, **c**) Group III, **d**) Group IV, **e**) Group V, and **f**) Group VI. Yellow, white, and red colored arrow indicates vascular degeneration, glial cell infiltration, and neuronal degeneration, respectively

crystal structure of various solid compounds. It is used to determine the degree of crystallinity. Amorphous material scatters at all wavelengths and gives a scattered pattern (continuous background); however, the crystalline material includes a crystal structure and produces definite diffraction lines or spots. The diffraction pattern of CSP revealed only one broad peak at 2θ values from 18.83 to 27.14° , and maximum peak height was obtained at 22.97° . Most of the prominent crystalline peaks often seen in diffraction patterns of CSE were not present in those of CSP. As a result of CSE phospholipid complex

formation, most of the crystalline peaks of CSE disappeared. Based on its diffraction pattern, CSP indicated that CSE in the Leciva S70 matrix might exist in either a molecularly distributed or amorphous form [39].

The optimized formulation followed a zero-order drug release kinetic model with a significance value of $P < 0.05$. The higher wettability and solubility of CSE in the prepared CSP formulation may account for the considerable difference in CSP release rate from CSE and PM. In the CSP formulation, CSE was changed from a crystalline to an amorphous state, which extended both the rate and

Table 5 Results of comparative bioavailability study after oral administration of CSE and CSP formulation

| Pharmacokinetic parameters | Treatment | |
|---|--------------------|------------------------|
| | CSE (250 mg/kg) | CSP (250 mg/kg of CSE) |
| C_{max} ($\mu\text{g/ml}$) | 0.404 ± 0.116 | 0.828 ± 0.134 |
| T_{max} (hours) | 1.71 ± 0.013 | 3.72 ± 0.018 |
| AUC 0-t ($\mu\text{g/ml} \cdot \text{h}$) | 2.492 ± 0.164 | 8.666 ± 0.186 |
| AUC 0-inf ($\mu\text{g/ml} \cdot \text{h}$) | 2.762 ± 0.119 | 8.864 ± 0.131 |
| $t_{1/2 ka}$ (hours) | 0.549 ± 0.123 | 1.867 ± 0.224 |
| V/F (mg/kg)/($\mu\text{g/ml}$) | 867.41 ± 0.019 | 300.74 ± 0.039 |
| CL/F (mg/kg)/($\mu\text{g/ml}$)/h | 180.99 ± 0.14 | 56.41 ± 0.124 |

* The information is shown as Mean \pm SD values ($n = 6$)

the extent of release over 12 h. The enhanced solubility of CSP was due to the amphiphilic nature of LECIVA S 70. The increased wettability and enhanced dispersion of CSP due to changes in the structural morphology of crystalline CSE into partial amorphization imparted due to the amphiphilic nature of LECIVA S 70 phospholipid [40]. There was no significant change in the CSP formulation during 6 months. However, a slight drop in EE and an increase in vitro release were detected throughout the storage period. This could be due to the release of drugs from the lipid matrix [20]. The temperature influences the lipid matrix over time, resulting in slender drug release from the interior and a modest increase in drug release. As the length of the storage period increased, slight increases in particle size and a slight decrease in zeta potential were observed. This could be attributed to the effect of temperature, which causes disturbances in the formed electrically double diffuse layer of formulation, but it could also be attributed to something else. Animals showed no clinical signs of intoxication at daily observations up to 14 days at a studied dose. Therefore, under the OECD 423 Guidelines and the specified laboratory circumstances, the LD50 value for CSP was determined to be >2000 – 5000 mg/kg body weight, placing it in GHS Category 5 and making it safe for use. CSP exhibited higher efficiency compared with CSE in MWMT, EPMT, and PCT. Administration of CSE, CSP, and piracetam for 15 consecutive days protected memory from memory impairment to different extents induced by scopolamine HBr. Hence, there was no observed increase in EL/TL even after the administration of scopolamine HBr on the 16th day. Thus, there was no significant practical effect on memory retention on the 16th day. Piracetam was used as a Positive control and showed significant improvements in memory in terms of EL/TL, as expected. Smaller particle size and the interaction

between phospholipid and CSE, which improves the overall hydrophilicity and solubility of CSE, may account for the relative absorption of CSP after oral administration. From this, we can infer that the EL/TL in MWMT, EPMT, and PCT were significantly lower in the CSP formulation-administered group compared to the CSE-administered group. Administration of CSP dose equivalent to pure extract (CSE) significantly increased the Ach level and inhibited Ach esterase activity. Acetylcholine is essential in controlling cognitive function in experimental and clinical settings. So CSP was more effective in increasing the level of Ach than CSE by decreasing the AchE activity [41, 42]. Dopaminergic neurons projecting from the substantia nigra to the striatum play a critical role in motor functions, while dopaminergic neurons originating in the ventral tegmental area (VTA) and projecting to the nucleus accumbens, hippocampus, and other cortical structures regulate rewarding learning [43]. Dopamine is the principal neurotransmitter involved in both the central nervous system (CNS) and peripheral nervous systems and plays a critical role in learning and memory. This release of dopamine helps us learn to associate the rewarding stimulus with the behavior that led to it [44]. Dopamine also plays a role in the consolidation of memories. This is the process by which memories are stored in the long term. When we learn something new, dopamine helps to strengthen the connections between the neurons that represent that information. This makes it more likely that we will be able to remember the information in the future. Dopamine levels are also important for working memory. This is a type of short-term memory that allows us to hold information in mind while we are working on a task. Dopamine helps keep information in working memory by increasing the activity of neurons in the prefrontal cortex. This allows us to focus on the task at hand and avoid distractions [45]. The prepared phytosome formulation (CSP) protects memory from scopolamine-induced memory impairment and enhances cognitive function by increasing dopamine concentration. A decline in DA concentration or inhibition of its synthesis or metabolism rates in the CNS can result in impairment of critical neurologic functions, such as cognition, behavior, and fine movements. The neurodegenerative disease often affects mental performance, particularly memory processes, and pathological changes have been reported to occur in the cholinergic, glutamatergic, serotonergic, and noradrenergic transmitter systems [45]. From these findings, it appears that several neurotransmitters are in some way involved in the formation and retrieval of memory traces. Measurement of cognitive performance in rats incorporates modulatory functions such as sensory, attentional, motivational, emotional, and motor processes. Serotonergic activity

has been linked to emotional processes and may play a particular role in emotional-related work. Serotonin, one of the most important neurotransmitters in the central nervous system, is synthesized by the amino acid tryptophan and is important in learning and memory. Indeed, 5-HT pathways, 5-HT reuptake site/transporter (SERT), and 5-HT receptors are present in brain areas implicated in learning and memory [46]. Serotonergic projections originate in the ascending raphe nuclei localized in the brain stem, where 5-HT synthesis, storage, and reuptake occur, and extend to almost all forebrain areas involved in learning and memory [47]. 5-HT exerts an influence via cholinergic and glutamatergic pathways over the transfer of information. Decreased brain serotonin levels impaired memory [48]. So, in this study, we found a significantly increased serotonin level in the CSP formulation-treated group as compared to the pure extract, which exhibited an increase in memory and learning. Acute and chronic central nervous system illnesses share the characteristics of neuroinflammation. Neuroinflammation is caused by glial cells like astrocytes and microglia being persistently activated in the brain and releasing inflammatory mediators such as cytokines, matrix metalloproteinases (MMPs), reactive oxygen species (ROS), and nitric oxide [10]. An unpaired t test was used to compare CSE and CSP results, and it was observed that the concentration of CSP was significantly ($p < 0.05$) greater than that of CSE. This demonstrates how CSE was delivered to the brain more effectively when it was a phyto-some formulation rather than a pure extract. This could be the result of phospholipid being present in phyto-somes, which might have changed GI permeability and prevented an apically directed efflux mechanism. It was found that the bioavailability of the CSP formulation was 3.21 times higher than that of the CSE formulation. Molecular aggregates and phospholipids work together to promote intestinal absorption and water solubility, which increases the plasma bioavailability of CSP after a single oral dosage.

Saima Rubab et al. also studied the neuropharmacological potential of various morphological parts of *C. sinensis* and it was observed that both leaves and seeds are active as neuropharmacological agents and can be used as memory-boosting agents. Neuropharmacological evaluation of seed and leaf extracts on mice revealed dose-dependent effects. Seed extract demonstrated significant stimulant activity, while leaf extract induced notable calmness and moderation. Tests including head dip, open field, and rearing showed increased motor function with both extracts, with leaf extract notably calming. Seed extract exhibited greater stimulant effects in cage cross, swimming, and traction tests. Leaf extract

showed similar effects but induced more calmness at higher doses. Micro-morphological investigation of *Camellia sinensis* is suggested for accurate identification. These findings highlight differing effects of plant parts, with seed extract being more stimulating and leaf extract inducing calming effects [49]. Similarly, Saima Rubab et al. performed phytochemical and pharmacological potential of *C. sinensis*. Both seed and leaf showed significant analgesic effects. However, compared to seed extract which showed highly significant ($p < 0.001$) increase in concentration dependent manner, leaf extract displayed highly significant results even at low dose with better results at high dose compared with standard [50, 51].

Muhammet Emin Cam et al. performed Morris's Water Maze Test to determine the potential of *C. Sinensis* leaves hydroalcoholic extract in AD. It was observed that the AD group reached the target quadrant later than the control group ($p < 0.05$) in all days and the total time spent in the quadrant decreased. In the MWM test, rats underwent spatial learning evaluation. Throughout training, all groups showed reduced time to locate the underwater platform, indicating learning. However, the Alzheimer's disease (AD) group exhibited prolonged training duration, indicating spatial memory impairment. Metformin treatment notably improved learning abilities, as evidenced by decreased training time compared to the AD group. Overall, the MWM test revealed enhanced spatial learning with metformin treatment, highlighting its potential therapeutic efficacy in cognitive decline associated with AD [52]. Similar observations were also noted in our experiments. The culmination of our investigation aligns with the outcomes observed by other research groups, affirming the potential efficacy of CSP formulation as a cognitive enhancer, surpassing the effects elicited by conventional CSE methodologies. This assertion is substantiated by a collective appraisal of research findings across various groups, suggesting a notable advantage conferred by CSP in enhancing memory functions.

Conclusion

Overall, the findings of this study suggest that the developed CSP formulation holds significant promise as a memory-enhancing agent, outperforming the effects of the conventional CSE. The observed improvements in memory, cognitive function, and bioavailability underscore the potential of nanophytosomes in enhancing the therapeutic properties of natural extracts for neurological applications. Further research and clinical studies are warranted to explore the translational potential of this CSP formulation in the context of cognitive disorders and related conditions.

Abbreviations

| | |
|------|-------------------------------------|
| CSE | <i>Camellia sinensis</i> Extract |
| CSP | <i>Camellia sinensis</i> Phytosomes |
| Ach | Acetylcholine |
| AD | Alzheimer's disease |
| EGCG | Epigallocatechin gallate |
| EE | Entrapment efficiency |
| CCD | Central composite design |
| PDI | Polydispersity index |
| DSC | Differential scanning calorimetry |
| PBS | Phosphate-buffered saline |
| EPMT | Elevated Plus Maze Test |
| MWMT | Morris Water Maze Test |
| CS | Conditioned stimulus |
| US | Unconditioned stimulus |

Supplementary Information

The online version contains supplementary material available at <https://doi.org/10.1186/s43094-024-00639-9>.

Additional file 1: Supplementary data. **Figure S1.** DSC thermogram: **a** CSE, **b** LECIVA, **c** PM and **d** CSP. **Figure S2.** SEM photomicrographs for optimized CSP. **Figure S3.** NMR Spectra: **a** CSE, **b** LECIVA, **c** CSP. **Table S1.** Stability study result of the CSP formulation.

Acknowledgements

For their assistance with this study, the authors are indebted to the Principal of Bharti Vidyapeeth College of Pharmacy at Kolhapur. In addition, the authors would like to extend their appreciation to Arjuna Remedies, Kerala, who generously sent a sample of their *Camellia sinensis* extract. The authors also want to thank Crystal Biological Solutions for all the help and support they gave them during the project. Finally, Chromeln, Pune Chromatographic Technology & Services are acknowledged for their assistance with HPLC analysis.

Author contributions

VM was involved in experimental work, writing/drafting manuscript. SK helped in design of experiments. HM and HT contributed to supervision of the project.

Funding

The present research work is not financially supported by any funding agency.

Availability of data and materials

The datasets generated during and/or analyzed during the current study are available from the corresponding author on reasonable request.

Declarations

Ethics approval and consent to participate

All animal handlings and experiments were approved by the Animal Ethical Committee of Crystal Biological Solution, Pune, with approval number CRY/2122/070.

Consent for publication

All authors agreed to publish the article in this journal.

Competing interests

The authors declare that they have no known competing financial interests or personal relationships that could have appeared to influence the work reported in this paper.

Author details

¹Bharati Vidyapeeth College of Pharmacy, Affiliated to Shivaji University, Kolhapur, Maharashtra 416013, India. ²Satara College of Pharmacy, Satara, Affiliated to Dr. Babasaheb Ambedkar Technological University, Lonere-Raigad, Maharashtra 402103, India. ³Anandi Pharmacy College, Kalambe Tarf Kale, Tal. Karveer, Dist. Kolhapur, Maharashtra 416205, India. ⁴Sharadchandra Pawar

College of Pharmacy, Otur, Affiliated to Savitribai Phule Pune University, Pune, Maharashtra 412409, India.

Received: 22 December 2023 Accepted: 21 April 2024

Published online: 01 May 2024

References

1. Rekatsina M, Paladini A, Piroli A, Zis P, Pergolizzi JV, Varrassi G (2020) Pathophysiology and therapeutic perspectives of oxidative stress and neurodegenerative diseases: a narrative review. *Adv Ther* 37:113–139. <https://doi.org/10.1007/s12325-019-01148-5>
2. Marchesi N, Fahmideh F, Boschi F, Pascale A, Barbieri A (2021) Ocular neurodegenerative diseases: interconnection between retina and cortical areas. *Cell* 10(9):2394. <https://doi.org/10.3390/cells10092394>
3. Huang Y, Lennart M (2012) Alzheimer mechanisms and therapeutic strategies. *Cell* 148(6):1204–1222. <https://doi.org/10.1016/j.cell.2012.02.040>
4. Lenègre A, Chermat R, Avril I, Stéru L, Porsolt RD (1988) Specificity of piracetam's anti-amnesic activity in three models of amnesia in the mouse. *Pharmacol Biochem Behav* 29(3):625–629. [https://doi.org/10.1016/0091-3057\(88\)90030-5](https://doi.org/10.1016/0091-3057(88)90030-5)
5. Logroscino G, Imbimbo BP, Lozupone M, Sardone R, Capozzo R, Battista P, Panza F (2019) Promising therapies for the treatment of frontotemporal dementia clinical phenotypes: from symptomatic to disease-modifying drugs. *Expert Opin Pharmacother* 20(9):1091–1107. <https://doi.org/10.1080/14656566.2019.1598377>
6. Karthivashan G, Ganesan P, Park SY, Kim J, Choi D (2018) Therapeutic strategies and nano-drug delivery applications in management of ageing Alzheimer's disease. *Drug Deliv* 25(1):307–320. <https://doi.org/10.1080/10717544.2018.1428243>
7. Junnuthula V, Kolimi P, Nyavanandi D, Sampathi S, Vora LK, Dyawanapelly S (2015) Polymeric micelles for breast cancer therapy: recent updates, clinical translation and regulatory considerations. *Pharmaceutics* 14(9):1860. <https://doi.org/10.3390/pharmaceutics14091860>
8. Atanasov AG, Waltenberger B, Pferschy-Wenzig E, Linder T, Wawrosch C, Uhrin P, Stuppner H (2015) Discovery and resupply of pharmacologically active plant-derived natural products: a review. *Biotechnol Adv* 33(8):1582–1614. <https://doi.org/10.1016/j.biotechadv.2015.08.001>
9. Holgate ST, Polosa R (2008) Treatment strategies for allergy and asthma. *Nat Rev Immunol* 8(3):218–230. <https://doi.org/10.1038/nri2262>
10. Szelenyi I, Brune K (2022) Herbal remedies for asthma treatment: between myth and reality. *Drugs Today* 38(4):265–303. <https://doi.org/10.1358/dot.2002.38.4.668337>
11. Jatwa V, Khirwadkar P, Dashora K (2014) Indian traditional memory enhancing herbs and their medicinal benefits. *IJRPB* 2(1):1030–1037
12. Habbu PTL, Hullatti P (2016) Phytosomes as novel drug delivery system for herbal medicine—a review. *Syst Rev Pharm* 8(1):5–7. <https://doi.org/10.5530/srp.2017.1.2>
13. Kolimi P, Narala S, Youssef AA, Nyavanandi D, Dudhipala N (2023) A systemic review on development of mesoporous nanoparticles as a vehicle for transdermal drug delivery. *Nanotheranostics* 7(1):70–89. <https://doi.org/10.7150/ntno.77395>
14. Mathur M (2016) Achievements, constraints and gaps of nano-techniques pertains to augmenting herbal drug efficacy. *Med Plants - Int J Phytomed Relat Ind* 8:171–198. <https://doi.org/10.5958/0975-6892.2016.00031.9>
15. Anjana R, Sunil K, Hitender S, Khar RK (2017) Phytosome drug delivery of natural products: a promising technique for enhancing bioavailability. *Int J Drug Deliv Technol* 7:157–65. <https://doi.org/10.25258/ijddt.v7i03.9559>
16. Khairnar SV, Pagare P, Thakre A, Nambiar AR, Junnuthula V, Abraham MC, Dyawanapelly S (2022) Review on the scale-up methods for the preparation of solid lipid nanoparticles. *Pharmaceutics* 14(9):1886. <https://doi.org/10.3390/pharmaceutics14091886>
17. Juneja LR, Chu D, Okubo T, Nagato Y, Yokogoshi H (1991) L-theanine—a unique amino acid of green tea and its relaxation effect in humans. *Trends Food Sci Technol* 10(6–7):199–204. [https://doi.org/10.1016/s0924-2244\(00\)00031-5](https://doi.org/10.1016/s0924-2244(00)00031-5)

18. Kaur T, Pathak CM, Pandhi P, Khanduja KL (2008) Effects of green tea extract on learning, memory, behaviour and acetylcholinesterase activity in young and old male rats. *Brain Cogn* 67:25–30. <https://doi.org/10.1016/j.bandc.2007.10.003>
19. Molino S, Dossena M, Buonocore D, Ferrari F, Venturini L, Ricevuti G, Verri M (2016) Polyphenols in dementia: from molecular basis to clinical trials. *Life Sci* 161:69–77. <https://doi.org/10.1016/j.lfs.2016.07.021>
20. Rathee S, Kamboj A (2018) Optimization and development of anti-diabetic phytosomes by box–benhken design. *J Liposome Res* 28(2):161–172. <https://doi.org/10.1080/08982104.2017.1311913>
21. Zhang J, Tang Q, Xu X, Li N (2013) Development and evaluation of a novel phytosomeloaded chitosan microsphere system for curcumin delivery. *Int J Pharm* 448:168–174. <https://doi.org/10.1016/j.ijpharm.2013.03.021>
22. Sze A, Erickson D, Ren L, Li D (2003) Zeta-potential measurement using the Smoluchowski equation and the slope of the current time relationship in electro osmotic flow. *J Colloid Interface Sci* 261:402–410. [https://doi.org/10.1016/s0021-9797\(03\)00142-5](https://doi.org/10.1016/s0021-9797(03)00142-5)
23. Telange DR, Patil AA, Pethe AM, Fegade H, Anand S, Dave VP (2017) Formulation and characterization of an apigenin-phospholipid phytosome (APLC) for improved solubility, in vivo bioavailability, and antioxidant potential. *Eur J Pharm Sci* 108:36–49. <https://doi.org/10.1016/j.ejps.2016.12.009>
24. Sutrisni NNW, Soewandhi SN, Adnyana IK, Sasongko L (2019) Acute and subchronic (28-day) oral toxicity studies on the film formulation of k-carrageenan and konjac glucomannan for soft capsule application. *Sci Pharm* 87(2):9. <https://doi.org/10.3390/scipharm87020009>
25. Kumar A, Dogra S, Prakash A (2009) Neuroprotective effects of *Centella asiatica* against intracerebroventricular colchicine induced cognitive impairment and oxidative stress. *Int J Alzheimers Dis* 9:972178. <https://doi.org/10.4061/2009/972178>
26. Abdelwahab GM, Mira A, Cheng Y, Abdelaziz TA, Lahloub MF, Khalil A (2021) Acetylcholine esterase inhibitory activity of green synthesized nanosilver by naphthopyrones isolated from marine-derived *Aspergillus niger*. *PLoS ONE* 16(9):e0257071. <https://doi.org/10.1371/journal.pone.0257071>
27. Yaguchi T, Nagata T, Nishizaki T (2009) 1-Palmitoyl-2-oleoyl-snglycerol-3-phosphocholine improves cognitive decline by enhancing long-term depression. *Behav Brain Res* 204:129–132. <https://doi.org/10.1016/j.bbr.2009.05.027>
28. Rat Dopamine, DA GENLISA™ ELISA, KRISHGEN BioSystems user manual.
29. Rat Serotonin, ST GENLISA™ ELISA, KRISHGEN BioSystems user manual.
30. Gupta S, Nair AB, Attimarad M (2020) Development and validation of bioanalytical method for the Determination of hydrazinocurcumin in rat plasma and organs by HPLC-UV. *J Chromatogr B Analyt Technol Biomed Life Sci* 1156:122310. <https://doi.org/10.1016/j.jchromb.2020.122310>
31. Zhang P, Chen L, Gu W, Gao Y, Li Y (2007) In vitro and in vivo evaluation of donepezil sustained release microparticles for the treatment of Alzheimer's disease. *Biomaterials* 28:1882–1888. <https://doi.org/10.1016/j.biomaterials.2006.12.016>
32. Asghar A, Raman AA, Daud WRW (2014) A comparison of central composite design and taguchi method for optimizing fenton process. *Sci World J* 188:1–14. <https://doi.org/10.1155/2014/869120>
33. Qin X, Yang Y, Fan T, Gong T, Zhang X, Huang Y (2010) Preparation, characterization and in vivo evaluation of bergenin-phospholipid complex. *Acta Pharmacol Sin* 31(1):127–136. <https://doi.org/10.1038/aps.2009.171>
34. Andersen SI, Jensen JO, Speight JG (2005) X-ray diffraction of subfractions of petroleum asphaltene. *Energy Fuel* 19(6):2371–2377. <https://doi.org/10.1021/ef050039v>
35. Danaei M, Dehghankhold M, Jenabi E, Davarani FH, Javanmard R, Dokhani A, Mozafari M (2018) Impact of particle size and polydispersity index on the clinical applications of lipidic nanocarrier systems. *Pharmaceutics* 10(2):57. <https://doi.org/10.3390/pharmaceutics10020057>
36. Savic R, Luo L, Eisenberg A, Maysinger D (2003) Micellar nanocontainers distribute to defined cytoplasmic organelles. *Science* 300:615–618. <https://doi.org/10.1126/science.1078192>
37. Semalty A, Semalty M, Singh D, Rawat MSM (2010) Preparation and characterization of phospholipid complexes of naringenin for effective drug delivery. *J Incl Phenom Macrocycl Chem* 67(3–4):253–260. <https://doi.org/10.1007/s10847-009-9705-8>
38. Yanyu X, Yunmei S, Zhipeng C, Qi-Neng P (2005) The preparation of silybin–phospholipid complex and the study on its pharmacokinetics in rats. *Int J Pharm* 307(1):77–82. <https://doi.org/10.1016/j.ijpharm.2005.10.001>
39. Karekar P, Killedar SG, Kulkarni S, Shaikh AY, Patil P (2023) Design and optimization of nanophytosomes containing mucuna prureins hydroalcoholic extract for enhancement of antidepressant activity. *J Pharm Innov* 18:310–324. <https://doi.org/10.1007/s12247-022-09646-w>
40. Dash S, Murthy PN, Nath L, Chowdhury P (2010) Kinetic modeling on drug release from controlled drug delivery systems. *Acta Pol Pharm* 67(3):217–223
41. Shayesteh S, Khalilzadeh M, Takzaree N, Dehpour AR (2022) Dapsone improves the vincristine-induced neuropathic nociception by modulating neuroinflammation and oxidative stress. *DARU J Pharm Sci* 30(2):303–310. <https://doi.org/10.1007/s40199-022-00448-6>
42. Jha MK, Jeon S, Suk K (2012) Glia as a Link between Neuroinflammation and Neuropathic Pain. *Immune Netw* 12(2):41–47. <https://doi.org/10.4110/in.2012.12.2.41>
43. Gopi C, Sastry VG, Dhanaraju MD (2019) Effect of novel phenothiazine derivatives on brain dopamine in Wistar rats. *Beni-Suef Univ J Basic Appl Sci* 8(1):1–9
44. Puig MV, Rose J, Schmidt R, Freund N (2014) Dopamine modulation of learning and memory in the prefrontal cortex: insights from studies in primates, rodents, and birds. *Front Neural Circ* 8:93. <https://doi.org/10.3389/fncir.2014.00093>
45. Myhrer T (2003) Neurotransmitter systems involved in learning and memory in the rat: a meta-analysis based on studies of four behavioral tasks. *Brain Res Rev* 41(2–3):268–287. [https://doi.org/10.1016/S0165-0173\(02\)00268-0](https://doi.org/10.1016/S0165-0173(02)00268-0)
46. Buhot MC, Martin S, Segu L (2000) Role of serotonin in memory impairment. *Ann Med* 32(3):210–221. <https://doi.org/10.3109/07853890008998828>
47. Mateos SS, Sánchez CL, Paredes SD, Barriga C, Rodríguez AB (2009) Circadian levels of serotonin in plasma and brain after oral administration of tryptophan in rats. *Basic Clin Pharmacol Toxicol* 104(1):52–59. <https://doi.org/10.1111/j.1742-7843.2008.00333.x>
48. Meneses A, Liy-Salmeron G (2012) Serotonin and emotion, learning and memory. *Rev Neurosci* 23(5–6):543–553. <https://doi.org/10.1515/revneuro-2012-0060>
49. Rubab S, Rizwani GH, Bahadur S, Shah M, Alsamadany H, Alzahrani Y, Alghamdi SA, Anwar Y, Shuaib M, Shah AA, Muhammad I (2020) Neuropharmacological potential of various morphological parts of *Camellia sinensis* L. *Saudi J Biol Sci* 27(1):567–573. <https://doi.org/10.1016/j.sjbs.2019.11.025>
50. Rubab S, Rizwani GH, Bahadur S, Shah M, Alsamadany H, Alzahrani Y, Alghamdi SA, Anwar Y, Shuaib M, Shah AA, Muhammad I (2020) Neuropharmacological potential of various morphological parts of *Camellia sinensis* L. *Saudi J Biol Sci* 27(1):567–573
51. Rubab S, Rizwani GH, Hassan M, Durrani AI, Hanif U, Ajaib M, Liaqat I, Sadiqa A, Shafi A, Batool FA (2022) Establishment of pharmacognostic standards of different morphological parts of *Camellia sinensis* L. grown in Pakistan. *Pak. J. Bot.* 54(4):1557–65
52. Muhammet Emin ÇAM, Turgut TAŞKIN (2020) *Camellia sinensis* leaves hydroalcoholic extract improves the alzheimer's disease-like alterations induced by type 2 diabetes in rats. *Clin Exper Health Sci* 10(2):93–103. <https://doi.org/10.33808/clinexphalthsci.685280>

Publisher's Note

Springer Nature remains neutral with regard to jurisdictional claims in published maps and institutional affiliations.